Contract No:

This document was prepared in conjunction with work accomplished under Contract No. DE-AC09-08SR22470 with the U.S. Department of Energy (DOE) Office of Environmental Management (EM).

Disclaimer:

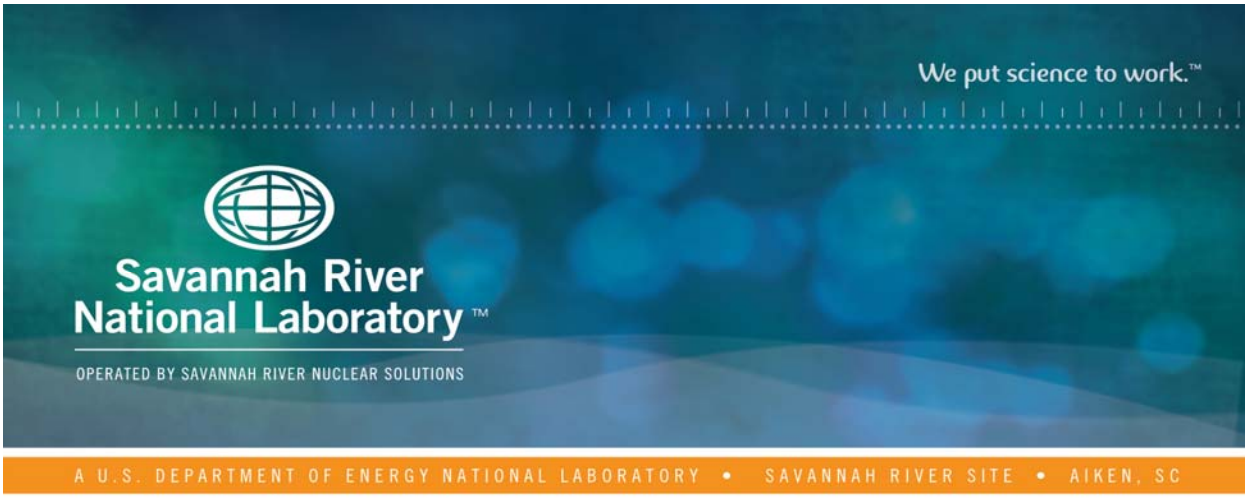

DWPF Nitric-Glycolic Flowsheet Chemical Process Cell Chemistry: Part 1

J. R. Zamecnik

T. B. Edwards

February 2016

SRNL-STI-2015-00681, Revision 0

DISCLAIMER

Printed in the United States of America

Prepared for
U.S. Department of Energy

SRNL-STI-2015-00681
Revision 0

Keywords: *DWPF, Chemical Processing Cell, Glycolic Acid*

Retention: *Permanent*

DWPF Nitric-Glycolic Flowsheet Chemical Process Cell Chemistry: Part 1

J. R. Zamecnik
T. B. Edwards

February 2016

Prepared for the U.S. Department of Energy under contract number DE-AC09-08SR22470.

Savannah River National Laboratory™
OPERATED BY SAVANNAH RIVER NUCLEAR SOLUTIONS

REVIEWS AND APPROVALS

AUTHORS:

approved by electronic signature *2/1/16*
J. R. Zamecnik, Process Technology Programs Date

approved by electronic signature *2/1/16*
T. B. Edwards, Engineering Process Development Date

TECHNICAL REVIEW:

approved by electronic signature *2/1/16*
J. D. Newell, Process Technology Programs, reviewed per E7 2.60 Date

approved by electronic signature *2/1/16*
H. L. Watson, Analytical R&D & Materials Characterization, reviewed per E7 2.60 Date

APPROVAL:

approved by electronic signature *2/1/16*
F. M. Pennebaker, Manager Date
Process Technology Programs

approved by electronic signature *2/1/16*
D. E. Dooley, Manager Date
Environmental & Chemical Process Technology Research Programs

approved by electronic signature *2/1/16*
E. J. Freed, Manager Date
Savannah River Remediation, DWPF & Salstone Engineering

Electronic Signatures:

Posted by
Jack Zamecnik
Entered on
02/01/2016

Generic Approval Routing

Tracking Number
GenAppr-2016-00002
Status: Approved

Title DWPF Nitric-Glycolic Flowsheet Chemical Process Cell Chemistry: Part 1

Attachments

SRNL-STI-2015-00681 rev 0.pdf

General Comment

New Comment

Submitted	Submitted By	Comment

Approval Routing: Approved on 02/03/2016

Approvers	Title	Assigned	Received	Status Changed	Status
Jack Zamecnik	Author1	02/01/2016 04:01:52 PM	02/01/2016 04:02:23 PM	02/01/2016 04:02:42 PM	Approved
Tommy Edwards	Author2	02/01/2016 04:01:52 PM	02/02/2016 06:25:55 AM	02/02/2016 06:26:16 AM	Approved
Holly Watson	Reviewer1	02/01/2016 04:01:52 PM	02/01/2016 04:02:39 PM	02/01/2016 04:05:04 PM	Approved
David Newell	Reviewer2	02/01/2016 04:01:52 PM	02/02/2016 10:31:48 AM	02/02/2016 10:31:58 AM	Approved
Frank Pennebaker	Manager PTP	02/01/2016 04:01:52 PM	02/01/2016 06:13:27 PM	02/01/2016 06:13:36 PM	Approved
David Dooley	Manager ECPT	02/01/2016 04:01:52 PM	02/01/2016 04:05:12 PM	02/03/2016 10:44:15 AM	Approved
Eric Freed	SRR	02/01/2016 04:01:52 PM	02/03/2016 10:55:23 AM	02/03/2016 02:18:17 PM	Approved

ACKNOWLEDGEMENTS

The authors would like to thank the numerous researchers and technicians whose work went into generating the data used in this work. They are too numerous to mention here.

EXECUTIVE SUMMARY

The conversions of nitrite to nitrate, the destruction of glycolate, and the conversion of glycolate to formate and oxalate were modeled for the Nitric-Glycolic flowsheet using data from Chemical Process Cell (CPC) simulant runs conducted by SRNL from 2011 to 2015. The goal of this work was to develop empirical correlations for these variables versus measureable variables from the chemical process so that these quantities could be predicted a-priori from the sludge composition and measurable processing variables. The need for these predictions arises from the need to predict the REDuction/OXidation (REDOX) state of the glass from the Defense Waste Processing Facility (DWPF) melter. This report summarizes the initial work on these correlations based on the aforementioned data. Further refinement of the models as additional data is collected is recommended.

The glass REDOX depends on the concentrations of nitrate and manganese (oxidants), and of glycolate, formate, oxalate, carbon, and antifoam (reductants) in the melter feed. The waste sludge contains nitrite, nitrate, Mn, and oxalate. Virtually all of the nitrite is converted to nitrate or $NO+NO_2+N_2O$ gases in the CPC. The portion of the nitrite converted to nitrate increases the amount of nitrate in the sludge. The amount of glycolate in the final melter feed depends on the amount of the glycolic acid feed that is destroyed. Similarly, the amounts of formate and oxalate formed during the decomposition of glycolic acid are required.

The nitrite to nitrate conversion expressed as the ratio of the final nitrate to the sum of the initial nitrite plus nitrate plus the nitric acid added (N_R) was found to correlate better with the variables than the actual nitrite to nitrate conversion value (N_C). Note that these two different ways to express conversion can be calculate from one another so use of the one with the best correlation was chosen. The variable N_R was found to be correlated and predicted reasonably well by the variables Headspace Volume to Sludge Volume (HSV), Acid Stoichiometry, and Percent Reducing Acid. Percent reducing acid is the fraction of the total nitric plus glycolic acids added that is glycolic acid. The HSV variable is a geometry dependent variable that appears to account for differences in internal reflux within the test vessels. Internal reflux is the condensation of evaporated water within the vessel, which is then returned (refluxed) directly back to the sludge. This internal refluxing has a greater effect in the 4-L simulant test vessels than in the larger test vessels because the HSV value is higher. DWPF performance is predicted to be similar to the larger scale vessels. The important point is that in the 4-L vessels where virtually all of the simulant tests are performed, the nitrite to nitrate conversion for a given set of variables will be higher than in larger scale tests and in DWPF. A recommended equation to predict nitrate in the products is proposed.

The glycolate destruction was found to correlate with HSV, Acid Stoichiometry, Percent Reducing Acid, and the initial nitrate, oxalate and iron concentrations in the sludge when data for multiple sludge compositions were regressed. The fit of the data to these variables was better than the fit of the nitrite to nitrate N_R variable, but the need for the many composition variables is somewhat questionable. Data from the Scaled Runs tests with a single sludge composition, which were the most highly controlled tests regarding composition measurements, result in correlation only with the Acid Stoichiometry. Three alternative equations are proposed for glycolate destruction. It is recommended that all three equations be used in future tests and the empirical models be further refined to determine the best equation.

The conversions of glycolic acid to formate and oxalate were found to be approximately constant when noble metals and mercury were present. The conversion to formate is about 0-2%, while the conversion to oxalate is about 2%. A value of 1% is recommended for formate. Oxalate values for older archived samples indicated higher conversions, but it appears that aging of the samples may increase the oxalate to concentrations higher than actually present immediately after test completion.

Further work is recommended to refine all of the models to generate better predictions. It is anticipated that both sludge batch independent and specific sludge batch models will be generated. The models generated for simulants will need to be further refined in DWPF using actual radioactive process data.

Because the chemistry of the glycolic acid reduction of sludge species is different than the chemistry with formic acid, it is recommended that further work be performed to better understand the actual chemistry so that an updated Minimum Acid Equation can be developed.

TABLE OF CONTENTS

LIST OF TABLES

LIST OF FIGURES

LIST OF ABBREVIATIONS

AS	Acid Stoichiometry
CPC	(DWPF) Chemical Process Cell
CQ	Caustic Quench (IC method)
CS	Calcine Solids
DWPF	Defense Waste Processing Facility
ELN	Electronic Laboratory Notebook
FTIR	Fourier Transform Infrared Spectroscopy or Spectrometer
GF	Glycolic-Formic
GN	Nitric-Glycolic
HSV	Headspace Volume to Sludge Volume
IC	Ion Chromatography
JMP	JMP statistical software package
KMA	Koopman Minimum Acid
MS	Mass Spectrometer or Spectrometry
NM	Noble Metals (& Hg) Present
OG	Offgas
PRA	Percent Reducing Acid
REDOX	REDuction OXidation
SASV	Surface Area (Headspace) to Sludge Volume
SB	Sludge Batch
SME	Slurry Mix Evaporator
SR	Scaled Runs (GN70-79)
SRAT	Sludge Receipt and Adjustment Tank
SRNL	Savannah River National Laboratory
TIC	Total Inorganic Carbon
WS	Without Scaled Runs Data
WU	Without Uncertain Data

1.0 Introduction

To implement the nitric-glycolic flowsheet in DWPF, adjustment of the Chemical Processing Cell (CPC) acid stoichiometry and of the reducing/oxidizing (glycolic/nitric) acid ratio to achieve a desired glass REDOX must be possible using only the incoming composition of the sludge. Note that the nitric-glycolic experimental data are abbreviated 'GN'. Glass REDOX (REDuction / OXidation) is the balance of reducing species to oxidizing species in the glass, e.g., Fe^{2+} vs. Fe^{3+}. The REDOX of the glass controls the deposition of metals that can short the joule-heating electrodes (too reducing) or increase the volatility of radionuclides such as Tc, Ru, and Cs (too oxidizing). The glass REDOX is dependent on the nitrate and glycolate concentrations and several other concentrations. The final nitrate and glycolate concentrations are dependent on the nitrite to nitrate conversion and the glycolate destruction percentages, which are not necessarily known a priori. In this work, data from simulant tests were analyzed and these percentages were regressed versus sludge composition variables, equipment configuration variables, and processing parameters that might be expected to affect these percentages. This report describes this work and proposes empirical correlations (models) for nitrite to nitrate conversion, glycolate destruction, and glycolate to formate conversion (when noble metals and mercury are not present). Recommendations for future work on these correlations and on the values input to them are made.

2.0 Experimental Data Utilized

The data used for this study were generated from multiple simulant CPC tests that occurred from 2011 to 2015. Some tests were complete SRAT/SME (see List of Abbreviations) cycles, some were only SRAT cycles, and some were SRAT cycles with frit added without performing an actual SME cycle. Early Alternate Reductant tests with both glycolic and formic acids were excluded from consideration. The applicability of any particular run was qualitatively judged by considering the values for the nitrate and glycolate anion concentrations and conversions during the test. Values judged to be unrealistic were excluded. The confidences of the anion analyses were judged to be high, medium, or low. Low values were excluded. The criteria for judging the confidence in the data were somewhat subjective. The reasonableness of the anion data, especially the glycolate analyses, was the primary criterion; values that gave glycolate destruction values that were far from values for similar runs were rated low. For some samples, as available, the slurry was reanalyzed for anions using the recently developed "caustic quench" (CQ) method.[1] These results were generally rated high, and the glycolate destruction values were also reasonable. The reproducibility of the anion analyses was also considered when qualitatively assigning the confidences. The descriptions of the simulant run data used are shown in Table 2-1.

The E7 2.60 review identified that some incorrect values were used in the empirical statistic models. These values included a few incorrect acid stoichiometry, percent reducing acid, Mn, Fe, and glycolate destruction values. The headspace parameters for all of the 4-L tests were found to be incorrect. There was insufficient time to re-regress all of the cases tested and update the results tables. The data regressions are compared by R^2 values that indicate how well the empirical model fits the data. When a sampling of the regressions were rerun with the corrected values, the resulting R^2 values differed by no more than ±0.01 in all but a few cases. These slight changes in values do not change the underlying conclusions made. In the following tables, the incorrect values that were used in the regressions are shown in parentheses next to or below the correct values. In the model fit comparison tables, the original R^2 values are shown. The individual regression output sheets are tabulated in ELN Experiment T7909-00035-13 and include the original and the corrected regressions for selected data sets; the corrected regressions are indicated with the letter 'a' after the name, e.g., glycolic destruction regression GdIC5a. The recommended regression equations to be used for predictions were updated to the corrected parameters.

Table 2-1. Description of Data Used for Models

Run Number	Anions Confidence	Cycles	Sludge Type	Scale (vessel volume L)	Acid Stoich (KMA)	Percent Reducing Acid	Noble Metals & Mercury	Run Series Description
GN34b	high	SRAT	HiFeHiMn	4	100%	63.00%	Yes	**Matrix Study** at High and Low Mn and Fe Concentrations
GN34c	high	SRAT	HiFeHiMn	4	104% (100%)	63.12%	Yes	
GN35	high	SRAT	LoFeHiMn	4	100%	56.89%	Yes	
GN36 SME	medium	SRAT / SME	HiFeLoMn	4	106%	59.25%	Yes	
GN36 SRAT	medium	SRAT / SME	HiFeLoMn	4	106%	59.25%	Yes	
GN36b	high	SRAT	HiFeLoMn	4	106%	59.25%	Yes	
GN36c	high	SRAT	HiFeLoMn	4	106%	59.25%	Yes	
GN37	medium	SRAT	LoFeLoMn	4	100%	60.42%	Yes	
GN37b	high	SRAT	LoFeLoMn	4	100%	60.26%	Yes	
GN38	high	SRAT	LoFeLoMn	4	125% (100%)	58.97%	Yes	
GN40	medium	SRAT / SME	2.0M Na SB8-B	4	130%	53.73% (50.66%)	Yes	**Less Washed Sludge** (SB8 type sludge)
GN41	high	SRAT / SME	2.5M Na SB8-B	4	130%	53.73%	Yes	
GN43	medium	SRAT	SB6J Blend	4	105%	51.89%	Yes	**Acid Stoichiometry Tests** (Blend of SB6 sludges used)
GN44	high	SRAT	SB6J Blend	4	85%	53.85%	Yes	
GN45	high	SRAT	SB6J Blend	4	95%	58.22%	Yes	
GN46	high	SRAT	SB6J Blend	4	90%	58.93%	Yes	
GN47	high	SRAT / SME	SB6J Blend	4	100%	56.37%	Yes	
GN48	high	SRAT / SME	SB6J Blend	4	100%	61.91%	Yes	
GN49	medium	SRAT / SME	SB6J Blend	4	100%	50.83%	Yes	
GN50	medium	SRAT / SME	SB6J Blend	4	100%	45.29%	Yes	
GN51	medium	SRAT (SME)*	SB6i	4	100%	54.64%	No	**Tests Supporting CEF Runs** (100% Acid Stoichiometry)
GN52	high	SRAT (SME)	SB6i	4	100%	55.14%	No	
GN53	high	SRAT (SME)	SB6i	4	125%	52.54%	No	
GN54	high	SRAT (SME)	SB6i	4	100%	51.03%	No	
GN55	high	SRAT (SME)	SB6i	4	100%	47.72%	No	
GN56	medium	SRAT (SME)	SB6i	4	100%	49.38%	No	
GN57	medium	SRAT (SME)	SB6i	4	110% (100%)	48.96%	Yes	Approximate comparison to GN56 with Noble Metals & Hg added
GN58	medium	SRAT (SME)	SB6i	4	125%	47.72%	No	**Tests Supporting CEF Runs** (125% Acid Stoichiometry)
GN59	medium	SRAT (SME)	SB6i	4	125%	45.97%	No	
GN70	high	SRAT / SME	SB8-D	4	100%	58.31%	Yes	**Scaled Runs**
GN71	high	SRAT / SME	SB8-D	4	125%	54.99%	Yes	
GN72	high	SRAT / SME	SB8-D	4	100%	52.09%	Yes	
GN73	high	SRAT / SME	SB8-D	4	110%	52.21%	Yes	
GN74	high	SRAT / SME	SB8-D	4	100%	54.54%	Yes	
GN75	high	SRAT / SME	SB8-D	4	110%	52.21%	Yes	
GN76	high	SRAT / SME	SB8-D	22	100%	58.31%	Yes	
GN77	high	SRAT / SME	SB8-D	22	110%	52.21%	Yes	
GN78	high	SRAT / SME	SB8-D	220	110%	52.21%	Yes	
GN79	high	SRAT / SME	SB8-D	220	100%	54.54%	Yes	

no noble metals or Hg | same sludge as 'no noble metals', but with noble metals and Hg | high Na tests

SRAT (SME)*: frit added without SME cycle

The GN30 series runs (originally called GF) samples were approximately 3 years old and were not originally analyzed using the caustic quench anions method. For several runs, two separate anion analysis results were used as distinct data points. All of the GN30 series samples were reanalyzed by the CQ method in 2015. However, some samples appeared to have lost glycolate while gaining oxalate, so these data are more uncertain. In the data analysis, these runs are referred to as “uncertain”. It is difficult to determine the extent of possible glycolate decomposition to form oxalate in the GN30 series because the original analyses were not done by the CQ method so the glycolate and oxalate values would be expected to be low in the original analyses. Higher values for glycolate by the CQ method were indeed found, but they might not have been as high as in the original product. Likewise, the CQ method gives higher oxalate, so it is unclear how much of the increase in the measured oxalate was from the better method and how much was from actual increases in concentration over time. A complete listing of the anion analyses is given in Appendix A.

From the anion analyses, the starting anion concentrations, and the amounts of nitric and glycolic acid added, the conversion of nitrite to nitrate and the destruction of glycolate were calculated using the acid calculation spreadsheet used for each run. The conversions of glycolate to formate and to oxalate are also

calculated. The destruction of glycolate was also calculated from the amount of CO_2 generated in the offgas. For most data, the anion concentrations at the end of the SRAT cycle were used to calculate these conversions since very little CO_2, NO_x, or NH_3 are generated in the SME cycle. The acid calculation spreadsheets are recorded in Experiment T7909-00035-13 in the Electronic Laboratory Notebook (ELN).

These conversions were empirically correlated to the variables shown in Table 2-2 using the JMP Pro Version 11.2.1 or JMP Version 11.2.0 statistical software.[2] There was insufficient variation in the quantities of noble metals and mercury used to include these as possible parameters in the regressions.

Table 2-2. Empirical Variables for Models

Empirical Variable	Abbreviation
Acid Stoichiometry (%) **	AS
Percent Reducing Acid (%)	PRA
Presence of Noble Metals & Mercury	NM
Initial Nitrite Conc. (mg/kg)	Nitrite
Initial Nitrate Conc. (mg/kg)	Nitrate
Initial Oxalate Conc. (mg/kg)	Oxalate
Fe Concentration (wt% calcine solids (CS))	Fe
Mn Concentration (wt% CS)	Mn
Headspace Surface Area to Sludge Volume Ratio (cm^{-1})	SASV
Headspace Volume to Sludge Volume Ratio	HSV

** Note that the acid stoichiometry was defined using the Koopman minimum acid (KMA) stoichiometry[3] equations for the nitric-formic acid flowsheet with glycolic acid substituted directly for formic acid on a molar basis. The actual correct minimum acid calculation for the nitric-glycolic flowsheet is not known, but using the KMA values serves as a way to compare runs. In the future, the new acid stoichiometry values can be substituted for the KMA values that are tabulated herein.

2.1 Quality Assurance

Requirements for performing reviews of technical reports and the extent of review are established in manual E7 2.60. SRNL documents the extent and type of review using the SRNL Technical Report Design Checklist contained in WSRC-IM-2002-00011, Rev. 2.

These reviews were conducted by J.D. Newell, H.L. Watson, and T.B. Edwards. Although a co-author, T.B. Edwards also performed part of this review on report parts that he was not directly involved in producing (specific calculations performed, and tables and figures generated independently by J.R. Zamecnik).

3.0 Results and Discussion

The conversion of nitrite to nitrate, the destruction of glycolate, and the formation of formate and oxalate from glycolate were calculated for each run using the acid calculation spreadsheet that is utilized for every CPC run. These values are summarized in Table 3-1.

Table 3-1. Variables Used in the Regressions

Run Number	Vessel Scale (L)	Surface Area to Sludge Volume Ratio (cm^{-1})	Headspace Volume to Sludge Volume Ratio	Acid Stoich. (KMA)	Percent Reducing Acid	Noble Metals & Mercury	Initial Nitrite mg/kg	Initial Nitrate mg/kg	Initial Oxalate mg/kg	Mn wt%CS	Fe wt%CS
GN34b	4	0.522 (0.542)	1.194 (1.401)	100%	63.00%	Yes	17900	13550	300	4.04	32.44
GN34c	4	0.522 (0.542)	1.191 (1.401)	104% (100%)	63.12%	Yes	17900	13550	300	4.04	32.44
GN35	4	0.523 (0.542)	1.197 (1.401)	100%	56.89%	Yes	9605	5880	7220	5.12 (3.08)	19.7 (10.54)
GN36	4	0.522 (0.542)	1.194 (1.401)	106%	59.25%	Yes	17800	13400	275	0.72	31.52
GN36b	4	0.522 (0.542)	1.194 (1.401)	106%	59.25%	Yes	17800	13400	275	0.72	31.52
GN36c	4	0.522 (0.542)	1.194 (1.401)	106%	59.25%	Yes	17800	13400	275	0.72	31.52
GN37	4	0.522 (0.542)	1.194 (1.401)	100%	60.42%	Yes	18100	13250	295	0.66	12.22
GN37b	4	0.518 (0.542)	1.176 (1.401)	100%	60.26%	Yes	18100	13250	295	0.66	12.22
GN38	4	0.517 (0.542)	1.17 (1.401)	125% (100%)	58.97%	Yes	18100	13250	295	0.66	12.22
GN40	4	0.49 (0.517)	1.106 (1.292)	130%	53.73% (50.66%)	Yes	13450	7895	18750	4.63	13.72
GN41	4	0.49 (0.517)	1.106 (1.292)	130%	53.73%	Yes	15750	9935	20000	4.23	12.41
GN43	4	0.576 (0.579)	1.336 (1.564)	105%	51.89%	Yes	12100	6595	387 *	7.09	17.80
GN44	4	0.576 (0.579)	1.336 (1.564)	85%	53.85%	Yes	12100	6595	387 *	7.09	17.80
GN45	4	0.576 (0.579)	1.336 (1.564)	95%	58.22%	Yes	12100	6595	387 *	7.09	17.80
GN46	4	0.577 (0.579)	1.338 (1.564)	90%	58.93%	Yes	12100	6595	387 *	7.09	17.80
GN47	4	0.456 (0.493)	1.016 (1.185)	100%	56.37%	Yes	12100	6595	387 *	7.09	17.80
GN48	4	0.456 (0.493)	1.016 (1.185)	100%	61.91%	Yes	12100	6595	387 *	7.09	17.80
GN49	4	0.456 (0.493)	1.015 (1.184)	100%	50.83%	Yes	12100	6595	387	7.09	17.80
GN50	4	0.456 (0.493)	1.015 (1.184)	100%	45.29%	Yes	12100	6595	387 *	7.09	17.80
GN51	4	0.471 (0.485)	1.054 (1.149)	100%	54.64%	No	9540	10600	781	7.08	22.20
GN52	4	0.471 (0.485)	1.054 (1.149)	100%	55.14%	No	9540	10600	781	7.08	22.20
GN53	4	0.471 (0.485)	1.057 (1.149)	125%	52.54%	No	9540	10600	781	7.08	22.20
GN54	4	0.471 (0.485)	1.054 (1.149)	100%	51.03%	No	9540	10600	781	7.08	22.20
GN55	4	0.471 (0.485)	1.054 (1.149)	100%	47.72%	No	9540	10600	781	7.08	22.20
GN56	4	0.471 (0.486)	1.055 (1.15)	100%	49.38%	No	9540	10600	781	7.08	22.20
GN57	4	0.468 (0.485)	1.042 (1.149)	110% (100%)	48.96%	Yes	9540	10600	781	7.08	22.20
GN58	4	0.471 (0.486)	1.055 (1.15)	125%	47.72%	No	9540	10600	781	7.08	22.20
GN59	4	0.471 (0.485)	1.054 (1.149)	125%	45.97%	No	9540	10600	781	7.08	22.20
GN70	4	0.454	1.011	100%	58.31%	Yes	12365	8102	2013	7.59	24.40
GN71	4	0.454	1.011	125%	54.99%	Yes	12365	8102	2013	7.59	24.40
GN72	4	0.454	1.011	100%	52.09%	Yes	12365	8102	2013	7.59	24.40
GN73	4	0.454	1.011	110%	52.21%	Yes	12365	8102	2013	7.59	24.40
GN74	4	0.454	1.011	100%	54.54%	Yes	12365	8102	2013	7.59	24.40
GN75	4	0.454	1.011	110%	52.21%	Yes	12365	8102	2013	7.59	24.40
GN76	22	0.094	0.395	100%	58.31%	Yes	12365	8102	2013	7.59	24.40
GN77	22	0.120	0.547	110%	52.21%	Yes	12365	8102	2013	7.59	24.40
GN78	220	0.108	0.887	110%	52.21%	Yes	12365	8102	2013	7.59	24.40
GN79	220	0.082	0.616	100%	54.54%	Yes	12365	8102	2013	7.59	24.40

no noble metals or Hg | same sludge as 'no noble metals', but with noble metals and Hg | high Na tests | * old value was 0

3.1 Headspace Variables

The variables Headspace Surface Area to Sludge Volume (SASV) and Headspace Volume to Sludge Volume (HSV) were chosen to potentially represent the region of the vapor headspace in the SRAT where internal refluxing could occur. Internal refluxing is the condensation of evaporated water as it cools in the headspace vapor or on the surfaces of the vessel headspace (walls, top head and components). It has been postulated that chemical reactions of offgas species occur in the headspace or on the surfaces of the headspace. The reactions most suspected of occurring are reactions of NO_x species with water to form nitrous and nitric acids that then condense and return to the SRAT vessel without the NO_x species actually ever leaving the vessel.

During acid addition, nitric oxide NO is the most likely offgas species formed directly from the decomposition of nitrite in the sludge. Some direct formation of NO_2 may also occur. The following reactions describe this chemistry.

SRAT liquid: $3\,HNO_2 \rightarrow HNO_3 + 2\,NO + H_2O$ [3.1]

Vapor space: $NO + \frac{1}{2}O_2 \rightarrow NO_2$ [3.2]

Vapor space or vapor space surfaces: $2NO_2 + H_2O \rightleftarrows HNO_2 + HNO_3$ [3.3]

Vapor space surface: $3\,HNO_2 \rightarrow HNO_3 + 2\,NO + H_2O$ [3.4]

The vapor space formation of nitrous and nitric acids is actually much more complex than indicated by Equation [3.3], but this equation summarizes the overall reactions occurring.

The reactions in Equations [3.3] and [3.4] also occur in the SRAT condenser, and during reflux, nitric acid is returned to the SRAT vessel. The formation and reflux of HNO_3 in the SRAT condenser and in the headspace are indistinguishable. SRAT condenser condensation composition measurements versus time would be needed to determine the amount of HNO_3 formed by internal refluxing. It has been assumed that the amount of scrubbing of NO_x in the SRAT condenser in the experimental tests was the same relative to the sludge volumes, so that there was no effect of scale on the relative amount of HNO_3 returned to the SRAT.

The reason for proposing an effect of the vapor headspace on the reactions was that there appeared to be differences in the nitrite to nitrate ratio in the Scaled Runs that correlated with the vessel size (4-L, 22-L, and 220-L). The actual volume of the vessel did not make sense as a variable affecting nitrite to nitrate conversion, so the variables SASV and HSV were proposed. HSV was proposed because it is the ratio of vapor headspace available for reactions [3.2]-[3.4] to the volume of sludge. The volume of sludge was used because it is the source term for the offgases, i.e., the amount of offgas species is dependent on the amount of sludge used. The SASV variable is the ratio of the headspace total surface area to the sludge volume and thus incorporates reactions [3.3]-[3.4] on the surfaces. In reality, the ‘variable’ that might be best for correlating the data could be some combination of these two variables. However, due to how scattered the data are, such distinctions were not possible.

The headspace surface areas and volumes for all of the GN runs and for DWPF are shown in Table 3-2. A summary of these calculations is given in Appendix B; the detailed calculations are archived in ELN Experiment T7909-00035-13. The headspace volume to sludge volume ratios and surface area to sludge volume ratios are plotted in Figure 3-1. Although these variables are smaller for the larger-vessel tests, this relationship is not necessarily a constant for a given size. For example, if the 4-L vessels used were filled significantly more, the amount of headspace could decrease to values like those for the larger vessels. The reason runs are not done this way is that overfilling results in much less vertical headspace for foam to dissipate and is thus not desirable from an operational standpoint.

Table 3-2. Headspace Surface Area and Volume Data

Vessel Size	Runs	Sludge Volume (mL)	Headspace Volume (mL)	Headspace Surface Area (cm^2)	Headspace Surface Area to Sludge Volume (SASV) (cm^{-1})	Headspace Volume to Sludge Volume (HSV)
DWPF	-	31,600,000	13,000,000	284,000	0.00901	0.411
220L	GN78	115,000	102,000	12,400	0.108	0.888
220L	GN79	134,000	82,700	11,100	0.0825	0.617
22L	GN76	17,600	6,960	1,660	0.0940	0.395
22L	GN77	15,900	8,690	1,900	0.120	0.547
4-L	GN70-75	3,040	3,070	1,380	0.454	1.01
		Average Values				
4-L	GN34-38	2,790	3,318	1,456	0.522	1.19
4-L	GN40-41	2,900	3,207	1,421	0.490	1.11
4-L	GN43-46	2,614	3,493	1,507	0.576	1.33
4-L	GN47-50	3,030	3,077	1,382	0.456	1.02
4-L	GN51-59	2,974	3,133	1,399	0.470	1.05

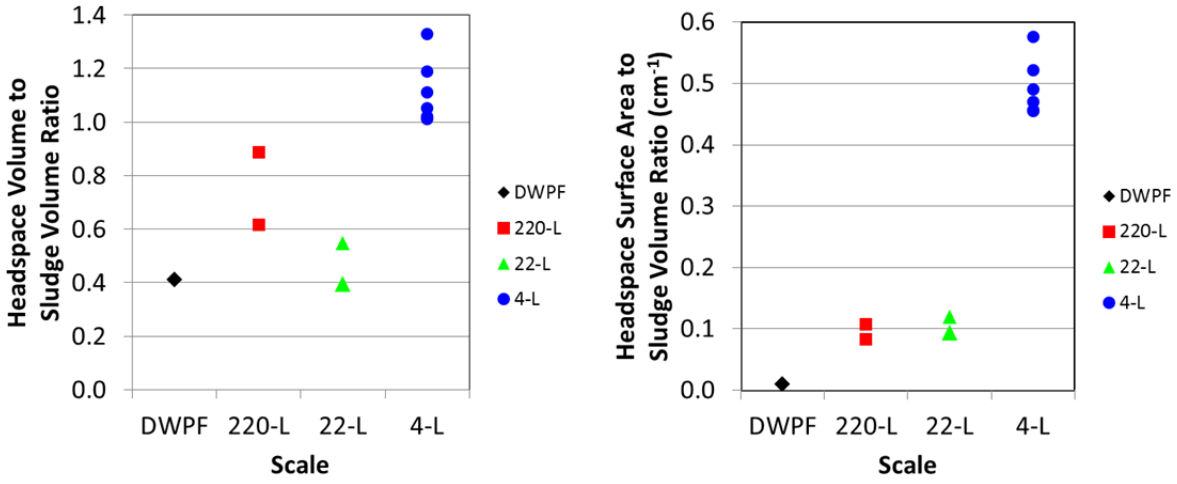

Figure 3-1. HSV and SASV for DWPF and Simulant Runs

Both HSV and SASV are significantly higher for the 4-L runs, meaning the headspace in these runs is a significantly larger portion of the vessel than in the larger vessels. The 4-L vessels are relatively tall and slender whereas the larger vessels have a height that is closer to the vessel diameter.

The variable HSV is similar for DWPF and the 22-L tests, while the 220-L values are higher but still only about half the 4-L values. If any conversions are truly proportional to HSV, then DWPF behavior would be expected to be similar to the 22-L runs.

The variable SASV is similar for the 22-L and 220-L runs and is about 1/5 of the values for the 4-L runs. Correlation to SASV would imply that the 22-L and 220-L vessels behaved similarly. However, the DWPF value is about 1/10 the 22- and 220-L values. This difference is significantly greater than the HSV values and would predict very different behavior in DWPF relative to the simulant test equipment. The reason the DWPF SASV value is so small is that SASV will always be smaller in a similarly configured larger vessel. SASV decreases by 1/radius whereas HSV is only dependent on the detailed dimensions and is not necessarily a function of the volume.

Since both of these variables are empirically derived to possibly capture the effect of different headspace geometries, there are no definitive reasons to pick one over the other.

3.2 Nitrite to Nitrate Conversion

The nitrite to nitrate conversion was calculated from the initial amount of nitrite and nitrate in the sludge and the amount of nitrate in the final product (SRAT or SME). Define nitrite to nitrate conversion N_C as:

$$N_C = \frac{n^P_{NO_3^-} - n^F_{NO_3^-} - n^{HNO_3}_{NO_3^-}}{n^F_{NO_2^-}}$$

where $n^P_{NO_3^-}$ = moles of nitrate in product

$n^F_{NO_3^-}$ = moles of nitrate in feed

$n^{HNO_3}_{NO_3^-}$ = moles of nitric acid added

$n^F_{NO_2^-}$ = moles of nitrite in feed

Alternatively, the fraction of the total original nitrite + nitrate + HNO_3 added that becomes nitrate N_R is:

$$N_R = \frac{n^P_{NO_3^-}}{n^F_{NO_3^-} + n^{HNO_3}_{NO_3^-} + n^F_{NO_2^-}}$$

where $n^P_{NO_3^-}$ = moles of nitrate in product

$n^F_{NO_3^-}$ = moles of nitrate in feed

$n^{HNO_3}_{NO_3^-}$ = moles of nitric acid added

$n^F_{NO_2^-}$ = moles of nitrite in feed

The quantity N_R can be thought of as the amount of nitrogen species that is not lost to the offgas system. This alternative formulation of the nitrite to nitrate conversion was found to correlate better with the proposed variables and still gives the needed conversion value. To calculate N_C from N_R:

$$N_C = \frac{(N_R - 1)\left(n^F_{NO_3^-} + n^{HNO_3}_{NO_3^-}\right) + n^F_{NO_2^-}}{n^F_{NO_2^-}}$$

To calculate N_R from N_C:

$$N_R = \frac{N_C n^F_{NO_2^-} + n^F_{NO_3^-} + n^{HNO_3}_{NO_3^-}}{n^F_{NO_3^-} + n^{HNO_3}_{NO_3^-} + n^F_{NO_2^-}}$$

These values for each run are tabulated in Table 3-3. The glycolate conversions are also shown. Glycolate destructions from offgas CO_2 values are only available for some runs; when unavailable, the table is marked NA. No nitrogen balances were specifically performed for this work. The nitrite to nitrate conversion values relied totally on the initial concentrations, the HNO_3 added, and the final nitrate concentration. Good closure (95-105%) of the nitrogen balances was found for the scaled runs,[4] so it is likely these balances would also be good for the other runs.

Table 3-3. Nitrite to Nitrate Conversion and Glycolate Destruction and Conversion Values

Run Number	Nitrite To Nitrate Conversion N_C	(Final Nitrate) to (Initial Nitrite + Initial Nitrate + Nitric Acid Added) Ratio	Glycolate Destruction (calculated from IC results)	Glycolate Destruction (calculated from offgas CO_2)	Glycolate Conversion to Oxalate	Glycolate Conversion to Formate and CO_2	(Glycolate to Formate + CO_2) to (Glycolate Destruction) Ratio
GN34b	43.2%	81.3%	28.8%	16.5%	8.4%	1.2%	4.1%
GN34c	38.2%	79.6%	25.0%	NA	9.1%	0.7%	2.8%
GN35	20.1%	78.1%	28.0%	NA	13.6%	2.1%	7.6%
GN36 SME	63.2%	90.2%	20.3%	20.2%	11.5%	1.8%	8.7%
GN36 SRAT	68.7%	90.2%	25.2%	20.2%	12.4%	1.8%	7.0%
GN36b	27.5%	77.3%	19.2%	NA	6.5%	0.7%	3.9%
GN36b	32.9%	78.9%	20.1%	NA	3.9%	0.0%	0.0%
GN36c	27.2%	77.2%	16.0%	NA	7.8%	0.8%	4.9%
GN37	40.8%	79.6%	31.3%	NA	4.3%	0.0%	0.0%
GN37b	21.7%	73.0%	17.6%	NA	6.4%	0.7%	4.0%
GN37b	19.9%	73.0%	9.8%	NA	3.4%	0.0%	0.0%
GN38	28.5%	78.2%	17.1%	10.9%	5.6%	1.1%	6.1%
GN40	66.5%	92.5%	16.3%	11.7%	2.5%	0.0%	0.0%
GN41	35.0%	83.9%	20.8%	NA	4.1%	1.1%	5.1%
GN43	52.8%	86.8%	28.5%	NA	1.4%	2.2%	7.9%
GN44	44.0%	81.9%	29.9%	17.2%	8.9%	6.7%	22.6%
GN45	51.8%	84.5%	21.9%	NA	2.8%	2.9%	13.0%
GN46	48.2%	82.7%	25.1%	18.3%	8.6%	1.6%	6.2%
GN47	31.2%	79.0%	26.3%	NA	5.6%	0.7%	2.6%
GN48	20.5%	73.9%	27.0%	NA	5.8%	0.6%	2.1%
GN49	40.9%	83.2%	35.1%	15.3%	5.4%	0.5%	1.5%
GN50	56.4%	88.4%	29.0%	NA	5.7%	0.5%	1.5%
GN51	5.8%	77.1%	28.0%	NA	5.3%	13.3%	47.6%
GN52	31.1%	83.2%	25.7%	NA	0.3%	13.6%	52.9%
GN53	27.2%	84.9%	20.7%	NA	0.6%	6.0%	29.0%
GN54	22.5%	82.0%	24.0%	NA	3.8%	14.4%	60.0%
GN54	27.4%	83.1%	25.0%	NA	0.7%	16.8%	67.4%
GN55	28.1%	83.9%	25.1%	NA	0.7%	17.6%	70.0%
GN56	62.1%	91.4%	24.3%	NA	0.0%	26.7%	100.0%
GN57	20.6%	83.6%	25.0%	NA	4.9%	0.7%	2.6%
GN58	58.9%	92.0%	20.8%	NA	0.3%	1.3%	6.0%
GN59	49.7%	90.4%	25.5%	NA	0.4%	1.5%	6.0%
GN70	23.3%	77.2%	17.6%	16.8%	1.5%	2.3%	13.0%
GN71	37.0%	84.4%	10.3%	11.2%	0.2%	1.5%	14.5%
GN72	26.5%	78.8%	19.9%	16.6%	0.3%	2.0%	9.9%
GN73	42.0%	84.9%	14.4%	11.6%	0.0%	1.2%	8.6%
GN74	31.6%	80.6%	20.5%	14.2%	0.0%	1.6%	8.0%
GN75	45.3%	85.8%	14.9% (13.6%)	13.1%	0.7%	1.3%	9.4%
GN76	17.5%	75.4%	20.4%	20.2%	2.1%	2.9%	14.0%
GN77	30.5%	81.9%	15.9%	14.4%	0.0%	1.3%	8.4%
GN78	23.8%	80.2%	16.5% (13.8%)	12.7%	0.1%	0.5%	3.3%
GN79	19.7%	77.2%	15.7%	17.6%	1.7%	0.9%	5.9%

no noble metals or Hg | same sludge as 'no noble metals', but with noble metals and Hg | high Na tests

The two formulations of nitrite to nitrate conversion, N_C and N_R, were regressed versus the variables in Table 3-1. The symbols used in JMP data analysis graphs are also shown. Data were regressed for the full set of data "All Data" and for several subset groupings of the data. The subsets used are shown in Table 3-5.

All runs performed prior to the Scaled Runs were done before the caustic quench (CQ) method for anion analysis was developed, so the glycolate and oxalate concentrations were questionable. As mentioned previously, the anion concentration values were judged somewhat subjectively to determine whether they could be used in the modeling. As many samples as possible were reanalyzed using the CQ method, but many were not available for reanalysis or were found to have significantly changed in solids content or appearance. As will be discussed later, it appears that some of the oldest (uncertain) samples may have had additional decomposition of glycolate and formation of oxalate over time.

Table 3-4. Description of Data Sets

Symbol	Data Set GN-	Sludge	Number of Data Points
∗	34-38 “Uncertain”	Hi/Lo Mn Fe “matrix”	11
□	40-41	High Na SB6-B	2
△	43-50 “Lower Acid Stoichiometry”	SB6J Blend	8
▽	51-56,58,59 “Without Noble Metals”	SB6I	8
△	57 (56 w/ noble metals & Hg)	SB6I	1
■	70-79 “Scaled Runs”	SB8D	10

Table 3-5. Data Subsets or Groupings

Data Description	Abbreviation
All Data	(ALL)
Without Uncertain Data (without 34-38)	(WU)
With Noble Metals & Hg (without 51-56,58,59)	(NM)
Without Noble Metals & Hg (51-56,58,59)	(woNM)
Scaled Runs Only	(SR)

For some test subsets, one or more of the parameters that were modeled did not vary significantly or at all, so that these parameters could not be used in the subset models, e.g., for the Scaled Runs, nitrite, nitrate, oxalate, Mn, and Fe did not vary.

3.2.1 Correlation of Experimental Parameters

Correlations between nitrite and nitrate and between Mn and Fe were found with the exception of certain data sets. The correlation of nitrite and nitrate is shown in Figure 3-2. For all data sets except GN51-59 (no noble metals), nitrite and nitrate were extremely correlated. This correlation is due to the tank farm maintaining an excess of nitrite relative to nitrate for corrosion control. The nitrite to nitrate ratios ranged from 1.32 to 1.83 except for GN51-59. In GN51-59, the ratio was 0.90. Because of this correlation, it is expected that any dependence of data on nitrite would have a similar dependence on nitrate. Only the data from GN51-59 would contribute any information to discerning a difference in dependence on nitrite versus nitrate. For the most part, a robust model would contain either nitrite or nitrate, but not both.

The correlation of Mn and Fe concentrations is shown in Figure 3-3. The Mn/Fe matrix data are shown in black and demonstrate the wide range of compositions tested. Only the composition at about 11% Fe and 3% Mn is an expected composition in a waste tank; the others were just extreme cases used to determine the effects of Mn and Fe separately from each other. The remaining data from all other runs are reasonably well correlated, so without the ‘Uncertain’ data, models depending on Mn or Fe should be fit about equally well with either parameter. Again, a robust model would not contain both Mn and Fe except when the ‘Uncertain’ data are included.

Based on the observed chemistry, a dependence on Mn is expected to be more likely than one on Fe because MnO_2 (Mn^{4+}) is known to be significantly reduced to Mn^{2+} whereas Fe^{3+} appears to be reduced much less to Fe^{2+}. (It has not yet been determined if solid Fe^{3+} species are being converted to solid Fe^{2+} species in the nitric-glycolic flowsheet.)

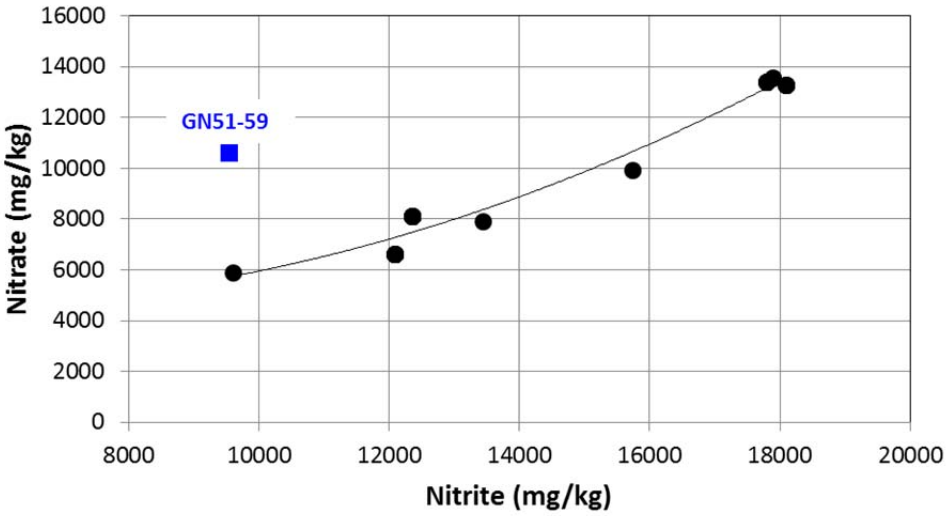

Figure 3-2. Correlation of Nitrite and Nitrate

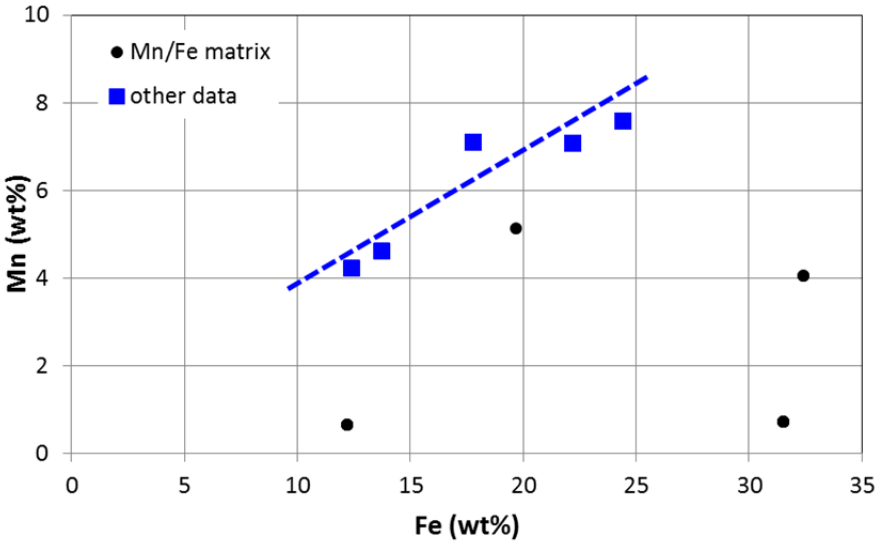

Figure 3-3. Correlation of Mn and Fe

3.2.2 General Formulation of Models

The models used for nitrite conversion to nitrate expressed either as N_C or N_R, glycolate destruction, glycolate conversion to formate + CO_2, and glycolate conversion to oxalate are empirical correlations of these data versus the variables in Table 2-2. The general progression for adding variables to the empirical models for the groups in Table 3-5 was:

1. Fit versus SASV or HSV, but not both.
2. Add acid stoichiometry (AS) and percent reducing acid (PRA).
3. Add additional linear parameters:
    a. Noble metals (NM)
    b. Nitrite

   c. Nitrate
   d. Oxalate
   e. Mn
   f. Fe
4. Remove nitrite or nitrate if both significant (since they are correlated).
5. Remove Mn or Fe if both significant (since they are correlated).
6. Add quadratic terms to account for possible nonlinearity or cross-terms (e.g., AS^2 or AS*PRA).

For subsets where a potential variable did not actually vary, the variable was excluded (e.g., for the Scaled Runs data, the nitrite, nitrate, oxalate, Mn, and Fe concentrations did not vary).

The stepwise regression feature of the Fit Model Platform in JMP was used to investigate for relationships between the explanatory variables and the responses of interest in this study. Two general types of models were considered: linear models, i.e., models with only linear terms as candidate effects and response surface models, whose candidate effects consisted of linear terms, squared terms, and two-way interaction terms.

For both types of models, stepwise regression (relying on JMP's p-value threshold stopping rule) was used to select a subset of the candidate effects to develop a regression model of potential interest. In general, the p-value for a term in a fitted model is a measure of the statistical significance: a small value (typically, less than or equal to 0.05) indicates a statistically significant term. JMP's default entrance p-value of 0.25 was used as the criterion for a candidate term to be considered during a forward step (JMP's default direction) of the fitting algorithm and subsequently to be entered into the model. Some cases were also performed using the combination of forward and backward (mixed) stepping when it was suspected that the forward stepping gave a sub-optimal result. Upon the completion of the stepwise routine, the "Make Model" feature available as part of the platform was used to fit the resulting model. The p-values for the active terms of the model were screened to remove any term whose p-value was above 0.20, unless the p-value was for a linear term which was also involved in a squared or two-way interactive term with an associated p-valve less than 0.20.

3.2.3 Modeling of Nitrite to Nitrate Conversion as N_C and N_R

The data were split into the categories shown in Table 3-5. The fit of the data as quantified by the R^2 value generally improved as the data sets were restricted to less data.

3.2.3.1 Nitrite to Nitrate Conversion as N_C

The R^2 values for fitting nitrite to nitrate conversion with SASV as a variable for All Data, All Data Without Uncertain (WU) data, and the Scaled Runs (SR) are shown in Table 3-7 along with a table indicating the significance of the variable in fitting the data. The significance is indicated by the color coding described in Table 3-6. The detailed JMP regression results can be found in ELN Experiment T7909-00035-13. The 'Identifier' field in the tables is used to identify the regression results in the appendix. Adjusted R^2 values are also shown in the tables.[1]

[1] The adjusted R-squared compares the descriptive power of regression models that include diverse numbers of predictors. Every predictor added to a model increases R-squared and never decreases it. Thus, a model with more terms may seem to have a better fit just for the fact that it has more terms, while the adjusted R-squared compensates for the addition of variables and only increases if the new term enhances the model above what would be obtained by probability and decreases when a predictor enhances the model less than what is predicted by chance. In an overfitting condition, an incorrectly high value of R-squared, which leads to a decreased ability to predict, is obtained. This is not the case with the adjusted R-squared.

Table 3-6. Color Codes for Significance of Variables in Models

Parameter Significance Prob. > |t|	Color
< 0.05	
< 0.10	
< 0.15	
< 0.20	
> 0.20	
> 0.20 but needed for quadratic term	
Not in model	
Not varied in data	

Table 3-7. Fit of Nitrite to Nitrate Conversion N_C to SASV and Additional Parameters

Data Set:		All Data					Without Uncertain Data					Scaled Runs	
Identifier:		**NCS1**	**NCS2**	**NCS3**	**NCS4**		**NCS5**	**NCS6**	**NCS7**	**NCS8**		**NCS9**	**NCS10**
R^2		0.26	0.38	0.47	0.56		0.38	0.59	0.77	0.80		0.78	0.92
R^2 adjusted		0.20	0.29	0.38	0.43		0.31	0.53	0.70	0.70		0.68	0.86
Surface Area/Sludge Volume	(SASV)												
Headspace Volume/Sludge Volume	(HSV)												
Acid Stoichiometry	(AS)												
Percent Reducing Acid	(PRA)												
Noble Metals Present	(NM)												
Nitrite (initial)													
Nitrate (initial)													
Oxalate (initial)													
Mn													
Fe													
Nonlinear (Quadratic) Terms					AS* PRA				AS* PRA	AS* PRA			SASV* AS
Nonlinear (Quadratic) Terms					nitrate^2				SASV* NM	SASV* NM			AS^2
Nonlinear (Quadratic) Terms					SASV* oxalate				AS* NM	AS* NM			
Nonlinear (Quadratic) Terms										SASV* oxalate			

Note: the Identifier row abbreviations are used in the appendix to identify the individual JMP data regression results.

The fit of N_C to SASV and additional variables is shown in Table 3-7. Column 1 (NCS1) shows that the fit versus only SASV with AS and PRA is very poor, with an R^2 value of only 0.26; AS and PRA were only marginally significant indicating that these parameters alone were insufficient. Columns 2 and 3 show adding additional variables but excluding nitrite improves the R^2 somewhat and PRA and NM are significant and AS and NM are somewhat significant. Adding both nitrite and nitrate improve the fit; NM becomes less significant and AS is no longer significant. Except for the No Noble Metals data, nitrite and nitrate are highly correlated, so most of the improvement in the fit from adding both is improving mostly the fit of the no NM data. The variables Mn and Fe are similarly correlated, with the only significant variations being in the Uncertain data.

Adding quadratic terms again improves the R^2. However, adding quadratic terms may only be improving the fit by just having more terms to describe data and not really capturing truly significant dependences. This is evident by the presence of the squared nitrate term without the nitrate term itself being significant. It was generally found that every additional variable added increased the R^2 by about 0.03.

The Uncertain data were then removed from the data set and the remaining data fit to similar models. The fits of the data improved relative to the complete data set. The linear model in column 6 has AS, PRA, and nitrate significant and an R^2 of 0.59. Again, the quadratic models improved the fit but the significance of the quadratic terms is questionable since AS became insignificant. Figure 3-4 shows the fit of the All Data and Without Uncertain data sets. The yellow highlighting shows that the linear model for all data does not fit the Uncertain Data points. No variables were found that could describe the difference in the Uncertain Data points, so the variation appears to be due to large measurement uncertainty in the nitrite and nitrate concentrations that go into calculating the nitrite to nitrate conversion. There were insufficient data (no offgas or condensate data) for these runs to perform complete nitrogen balances over the system. The 95% confidence interval on the predicted values is shown by the dotted red lines in these plots.

The Scaled Runs data, which had the best control and measurements of the product compositions, have much higher R^2 values. The linear model (column 10 in Table 3-7) has an R^2 of 0.78 with both AS and PRA being somewhat significant. The fact that AS and PRA are only significant at <0.10 shows that AS and PRA cannot completely account for the variations in the data. The quadratic model has R^2 equal to 0.92; the addition of the cross term SASV*AS and the AS^2 term make sense since these variables are also present as linear terms. The somewhat significant PRA is no longer significant. The interaction term SASV*AS does not seem to have a physical meaning, but the AS^2 term may suggest that the dependence of the nitrite to nitrate conversion is nonlinear. With complex chemical kinetics, there is no reason to believe that only linear effects would be significant, but cross terms are probably less likely. In general, including many variables in an empirical model even if statistically significant can just be fitting the noise or random variation in the data. Therefore, linear models with the least number of parameters are more likely to incorporate the most important and physically meaningful variables.

The variables that were most consistently significant for the All Data and Without Uncertain Data sets, in addition to SASV, were PRA and nitrate, with Fe (or Mn) also being significant for All Data (due to the inclusion of Uncertain data). The effect of NM was probably correlated with the nitrite and nitrate since this is the only data set that had a significantly different ratio of nitrite to nitrate. The effect of AS was somewhat significant in most of the models.

Plots of the WU data and the SR data are shown in Figure 3-5. The fit of the SR data by itself is much better than the fit with the WU data. It is apparent that the individual fit of the SR data is very similar to the fitted values for this subset of data in the WU model. Figure 3-6 shows a comparison of the linear and quadratic fits of the Scaled Runs data.

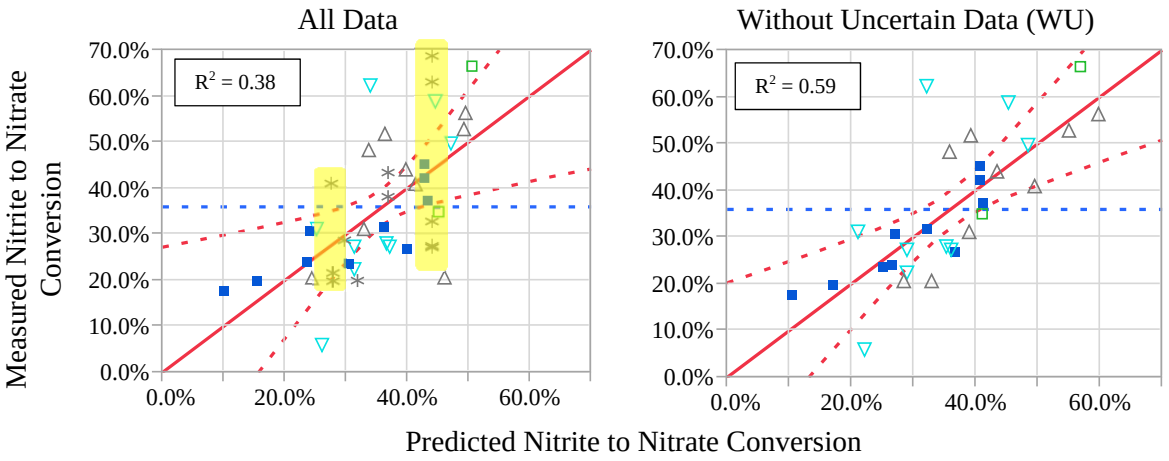

Figure 3-4. Comparison of Nitrite to Nitrate Fits to SASV

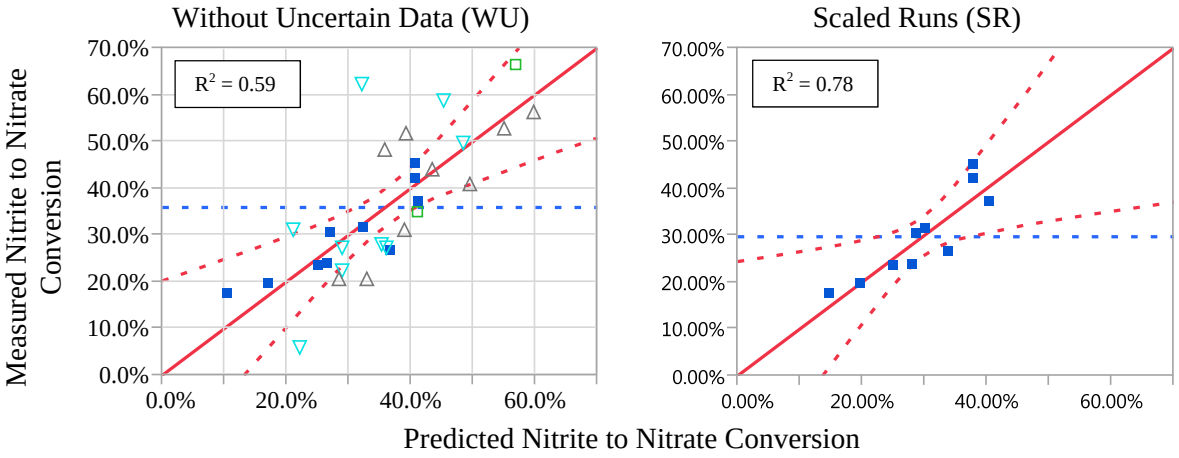

Figure 3-5. Comparison of Nitrite to Nitrate Fits to SASV

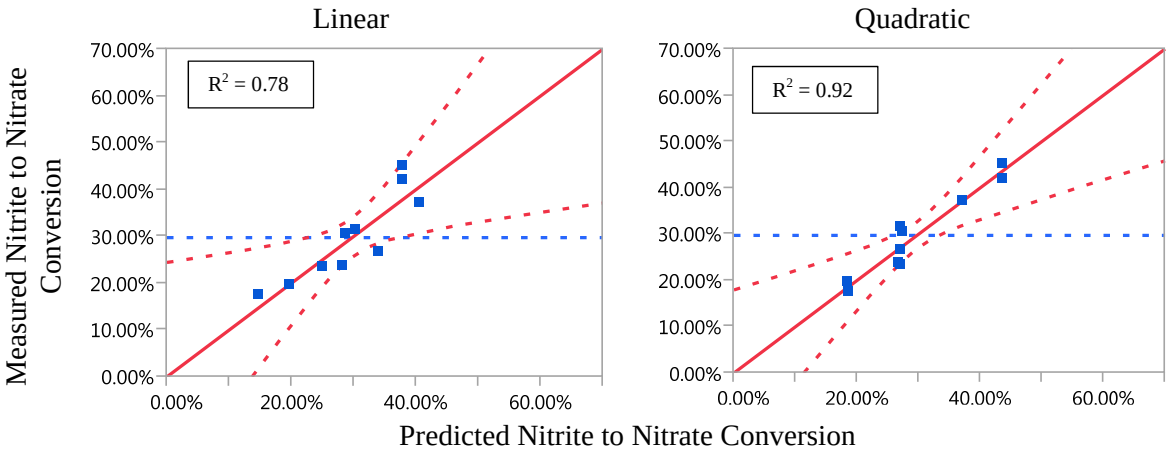

Figure 3-6. Comparison of Nitrite to Nitrate Fits to SASV for Scaled Runs Data

The fits of these same data to the HSV variable are shown in Table 3-8. The fits of all data are very similar to the results using the SASV variable. Both linear models of All Data have R^2 values of 0.47 with PRA, nitrite, nitrate, and Fe significant and NM somewhat significant. The data without the uncertain data are fit similarly well to both SASV and HSV. The data without the uncertain data and also without the no noble metals data (all noble metals data without uncertain data) were also fit to a linear model. The R^2 for this more restricted data set (column 11) was 0.77 versus 0.59 when the no NM data is included. The no NM data appear to have significantly more scatter than the remaining data; the model variables were unable to account for this scatter, indicating that it was also 'more uncertain' than the other data. All data with NM and data without NM were also fit to linear models as shown in columns 14-16. The without NM data appear to be fit better, but the R^2 adjusted value shows this is not really true.

The Scaled Runs data are fit significantly poorer using HSV than with SASV. With the HSV data, the PRA is never significant, and for the linear model HSV and AS are only marginally significant. These results for the SR data indicate that HSV is not the headspace variable to use to correlate the nitrite to nitrate ratio.

Table 3-8. Fit of Nitrite to Nitrate Conversion N_C to HSV and Additional Parameters

Data Set:		All Data						
Identifier:		NCH1	NCH2	NCH3	NCH4	NCH5	NCH6	NCH7
R^2		0.29	0.40	0.40	0.43	0.47	0.48	0.52
R^2 adjusted		0.24	0.32	0.32	0.33	0.38	0.37	0.43
Surface Area/Sludge Volume	(SASV)							
Headspace Volume/Sludge Volume	(HSV)							
Acid Stoichiometry	(AS)							
Percent Reducing Acid	(PRA)							
Noble Metals Present	(NM)							
Nitrite (initial)								
Nitrate (initial)								
Oxalate (initial)								
Mn								
Fe					>0.2			
Nonlinear (Quadratic) Terms							HSV* oxalate	AS* PRA
Nonlinear (Quadratic) Terms							PRA* Fe	nitrite^2

Data Set:		Without Uncertain Data			
					w/o no NM Data
Identifier:		NCH8	NCH9	NCH10	NCH11
R^2		0.42	0.59	0.64	0.77
R^2 adjusted		0.35	0.53	0.57	0.71
Surface Area/Sludge Volume	(SASV)				
Headspace Volume/Sludge Volume	(HSV)				
Acid Stoichiometry	(AS)				
Percent Reducing Acid	(PRA)				
Noble Metals Present	(NM)				
Nitrite (initial)					
Nitrate (initial)					
Oxalate (initial)					
Mn					
Fe					
Nonlinear (Quadratic) Terms				AS* PRA	

Data Set:		Scaled Runs		With NM		Without NM
Identifier:		NCH12	NCH13	NCH14	NCH15	NCH16
R^2		0.63	0.68	0.33	0.42	0.50
R^2 adjusted		0.45	0.53	0.26	0.33	0.19
Surface Area/Sludge Volume	(SASV)					
Headspace Volume/Sludge Volume	(HSV)					
Acid Stoichiometry	(AS)					
Percent Reducing Acid	(PRA)					
Noble Metals Present	(NM)					
Nitrite (initial)						
Nitrate (initial)						
Oxalate (initial)						
Mn						
Fe						
Nonlinear (Quadratic) Terms			AS^2			

3.2.3.2 Nitrite to Nitrate Conversion as N_R

The results of fitting the nitrite to nitrate conversion expressed as N_R are shown in Table 3-9 for SASV as the vapor space variable.

Table 3-9. Fit of Nitrite to Nitrate Conversion N_R to SASV and Additional Parameters

Data Set:		**All Data**			**Without Uncertain Data**		**Scaled Runs**			
Identifier:		**NRS1**	**NRS2**	**NRS3**	**NRS4**	**NRS6**	**NRS7**	**NRS8**	**NRS9**	**NRS10**
R^2		0.55	0.62	0.66	0.74	0.81	0.90	0.90	0.985	0.997
R^2 adjusted		0.51	0.58	0.61	0.71	0.77	0.84	0.85	0.955	0.985
Comparison Identifier:		NCS1	NCS3	NCS4	NCS5	NCS7	NCS9	NCS10	NCS10	NCS10
Value for fit of N_C: R^2		0.26	0.47	0.56	0.38	0.77	0.78	0.92	0.92	0.92
Surface Area/Sludge Volume	(SASV)									
Headspace Volume/Sludge Volume	(HSV)									
Acid Stoichiometry	(AS)									
Percent Reducing Acid	(PRA)									
Noble Metals Present	(NM)									
Nitrite (initial)										
Nitrate (initial)										
Oxalate (initial)										
Mn										
Fe										
Nonlinear (Quadratic) Terms				SA^2		SASV*nitrate		AS^2	AS^2	AS^2
Nonlinear (Quadratic) Terms									SA* PRA	SA* AS
Nonlinear (Quadratic) Terms									PRA^2	PRA^2
Nonlinear (Quadratic) Terms										$SASV^2$

The fit of the data expressed in terms of N_R is significantly better than the corresponding fits for N_C as shown in the table. Again, the fit without the Uncertain data is much better than All Data, and the Scaled Runs data fit is even better. For All Data and WU data, both AS and PRA are significant, whereas for fitting N_C, AS was marginally significant and PRA varied from significant to somewhat significant. As with the fit of N_C, the Fe was significant when the Uncertain data were included. Nitrate, significant in some N_C models, was only marginally significant in the quadratic model for the WU data. Less significant variables and better R^2 values indicate that the fitting of N_R is better than N_C. Plots of the measured versus predicted values similar to Figures 7–9 are shown in Figures 10–12. The linear fit of the SR data by itself is very similar to the fit of these data points in the WU data set. The quadratic fit of SR data is extremely good, but it uses 7 variables to fit 10 data points; it is not likely that the same parameter values in this fit would still apply if more data points were added, i.e., it is over-specified. However, for additional SR runs, it would be expected that any of the SR models would give a good prediction for additional runs.

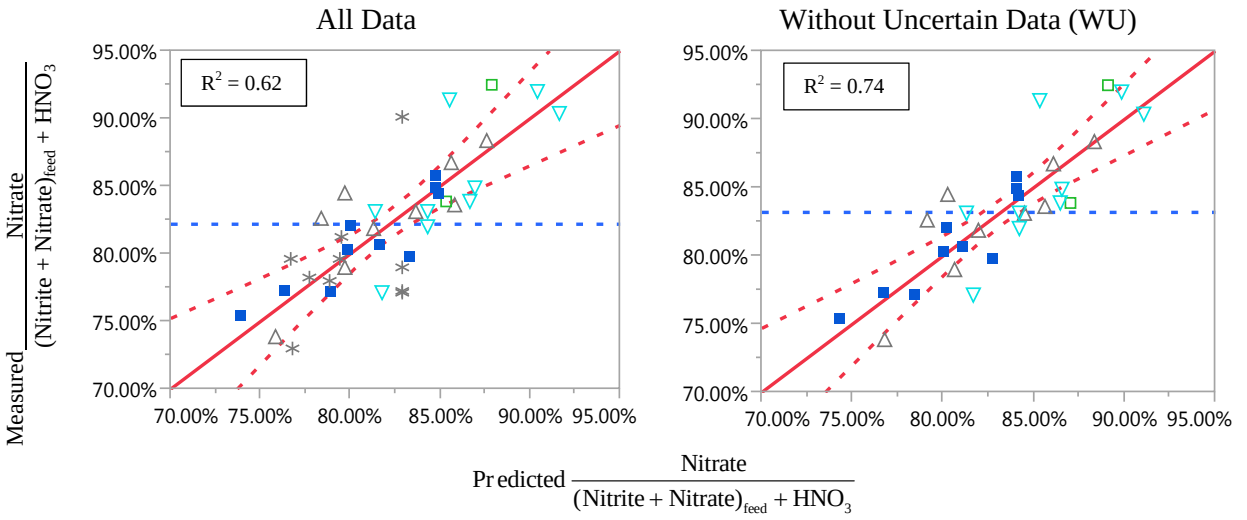

Figure 3-7. Comparison of Nitrite to Nitrate Fits to SASV

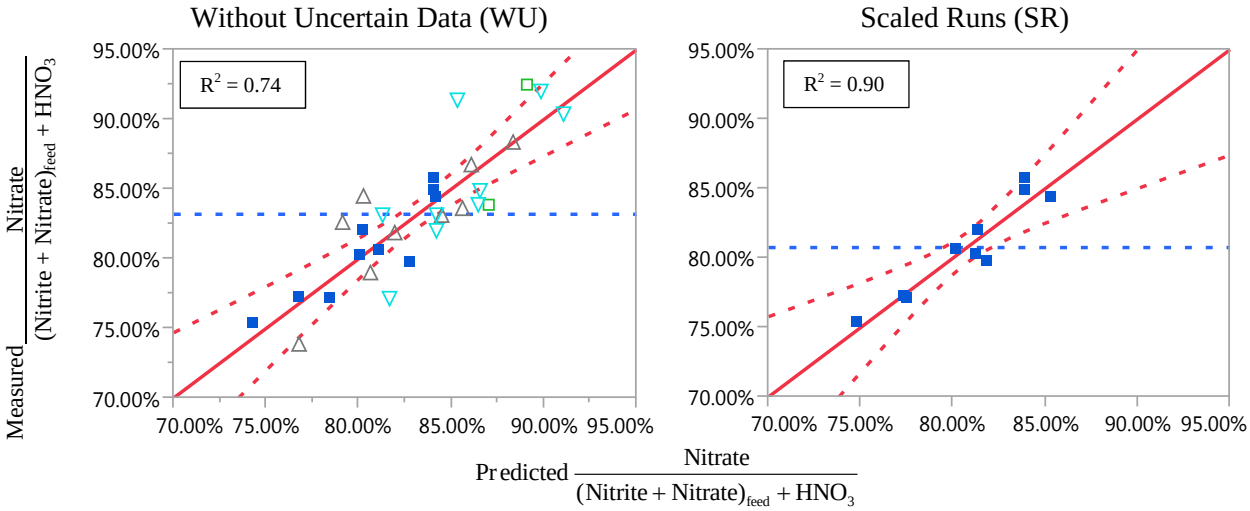

Figure 3-8. Comparison of Nitrite to Nitrate Fits to SASV

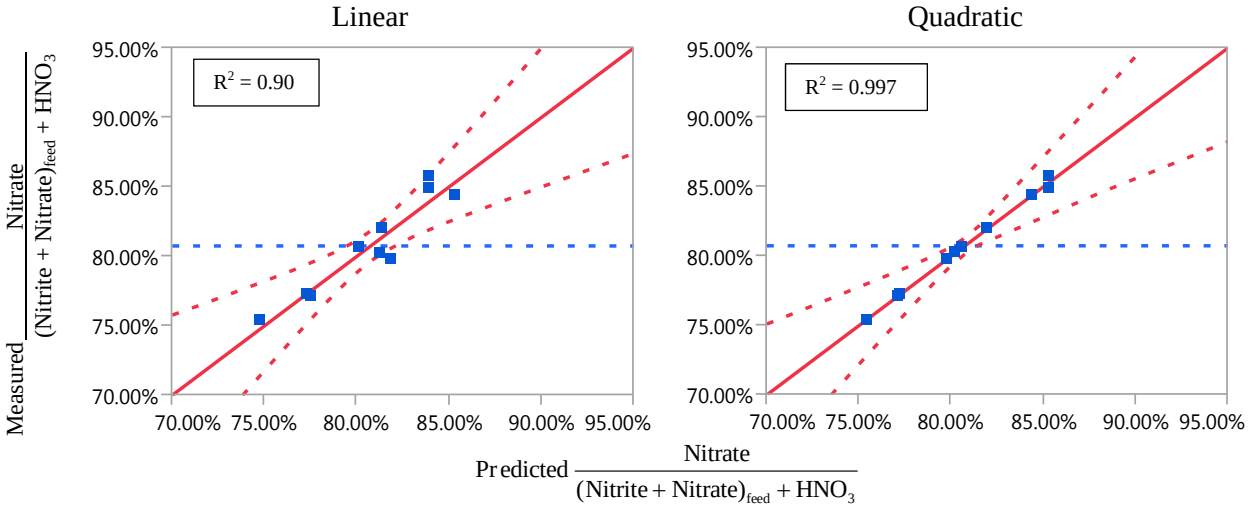

Figure 3-9. Comparison of Nitrite to Nitrate Fits to SASV for Scaled Runs Data

Table 3-10. Fit of Nitrite to Nitrate Conversion N_R to HSV and Additional Parameters

Data Set:		All Data			Without Uncertain Data			Scaled Runs		
Identifier:		NRH1	NRH2	NRH3	NRH4	NRH5	NRH6	NRH7	NRH8	NRH9
R^2		0.56	0.63	0.66	0.75	0.78	0.83	0.75	0.82	0.88
R^2 adjusted		0.52	0.59	0.61	0.72	0.74	0.77	0.67	0.73	0.78
Comparison Identifier:		NCH1	NCH5	NCH7	NCH8	NCH10	NCH10	NCH12	NCH12	NCH13
Value for fit of N_R: R^2		0.29	0.47	0.52	0.42	0.64	0.64	0.63	0.63	0.68
Surface Area/Sludge Volume	(SASV)									
Headspace Volume/Sludge Volume	(HSV)									
Acid Stoichiometry	(AS)									
Percent Reducing Acid	(PRA)									
Noble Metals Present	(NM)									
Nitrite (initial)										
Nitrate (initial)										
Oxalate (initial)										
Mn										
Fe										
Nonlinear (Quadratic) Terms				HSV^2		HSV^2	HSV^2			HSV^2
Nonlinear (Quadratic) Terms							HSV* PRA			
Nonlinear (Quadratic) Terms							PRA* Mn			

Table 3-10 shows the results of fitting N_R to the HSV variable. Compared to the values in Table 3-9, the fits of All Data and WU data have very similar results, indicating that for these data sets there is no reason to pick HSV versus SASV. However, for the Scaled Runs data only, the fits versus HSV are not nearly as good as the fits versus SASV. HSV is only somewhat to marginally significant, indicating that this variable cannot account for much of the variation. Recall that HSV was also not as significant in the N_C models.

The R^2 values for the nitrite to nitrate models are summarized in Table 3-11. The fits of N_R are always better than the corresponding fit of the N_C data. For All Data or the WU data, the addition of SASV or HSV introduces approximately equivalent improvements in the R^2 values.

However, for the Scaled Runs data, SASV introduces the greatest improvement. The fits of N_C and N_R for the Scaled Runs without SASV and HSV have been added to Table 3-11. For the Scaled Runs data, the addition of SASV is seen to improve the fits more than the addition of HSV for both representations of the nitrite to nitrate conversion. N_C is improved more by adding either of these variables. Even though HSV is not significant at the 0.05 level, its inclusion improves all of the SR models' R^2 values by at least 0.07, and so HSV should be included in modeling these data.

Table 3-11. Summary of R^2 Values for Nitrite to Nitrate Models

		All Data			Without Uncertain Data			Scaled Runs	
Model	**Vapor Space Term**	**Linear (AS, PRA only)**	**Linear (all variables*)**	**Quadratic**	**Linear (AS, PRA only)**	**Linear (all variables*)**	**Quadratic**	**Linear (AS, PRA only)**	**Quadratic**
N_C	none	-	-	-	-	-	-	0.49	-
	SASV	0.26	0.38 - 0.47	0.56	0.38	0.59	0.77 - 0.80	0.78	0.92
	HSV	0.29	0.40 - 0.47	0.48 - 0.52	0.42	0.59	0.64	0.63	0.68
N_R	none	-	-	-	-	-	-	0.75	-
	SASV	0.55	0.62	0.66	0.74	0.74†	0.81	0.90	0.90 - 0.997
	HSV	0.56	0.63	0.66	0.75	0.78	0.83	0.82	0.88

* all *significant* variables † same as AS, PRA only (no additional significant variables)

It would be expected that the best data to test the dependence on HSV or SASV would include data from the scaled runs since the 22- and 220-L runs had values that differed from the 4-L runs. Averages of the HSV and SASV variables from Table 3-2 are shown in Table 3-12. The ratios of the HSV and SASV values to the average values for the 4-L runs are also shown. For HSV, predictions of DWPF values would be similar to the predictions for the 22-L runs, since the ratio values are similar. However, for SASV the DWPF ratio is an order of magnitude lower than the 22- and 220-L runs and two orders of magnitude lower than the 4-L runs. Because there is no data for SASV values around 0.01, extrapolation of the model values to DWPF using the SASV variable would be risky.

Table 3-12. Headspace Surface Area and Volume Data

Vessel Size	**Runs**	**Headspace Surface Area to Sludge Volume (SASV) (cm^{-1})**	**SASV / $SASV_{4L}$**	**Headspace Volume to Sludge Volume (HSV)**	**HSV / HSV_{4L}**
DWPF	-	0.00901	0.018	0.411	0.37
220-L	GN78-79	0.0951	0.19	0.752	0.67
22-L	GN76-77	0.107	0.22	0.471	0.42
4-L	GN34-75	0.494	1	1.12	1

Examination and comparison of the estimated parameter values in the prediction equations can help interpret the relative importance of each variable in the prediction equations. The estimated parameter values for models of All Data without both Uncertain and Scaled Runs, without Uncertain, and Scaled Runs alone for both HSV and SASV are shown in Table 3-13 along with typical values for the variables. The coefficients apply this equation: $N_R = I + a*SASV + b*AS + c*PRA$ .These data are for linear fits with variables SASV or HSV, AS, and PRA. The data were also regressed against All Data without Uncertain *and* without SR data so that the effect of the SR data on the overall values could be demonstrated. Note that the coefficients on SASV and HSV are largest when the SR data are not present. For example, for SASV the value without the SR data is 0.34, decreasing to 0.12 when the SR data are added back in, and again decreasing to 0.08 for the SR data alone. These results indicate that when the more varied SR data are included, the dependence on SASV or HSV actually decreases. This also means that the variations in N_R in the WU data set due to SASV or HSV are not as accurately described because the lower SR data set values leverage the parameter more.

Table 3-13. Coefficients of Linear Prediction Equations for N_R

		SASV						HSV						
					Typical Variable Value						Typical Variable Value			
Term	Coeffi-cient	Without Uncertain & Scaled Runs (WU/WS) (NRS12)	Without Uncertain (WU) (NRS4)	Scaled Runs (SR) (NRS7)	4L	22 or 220L	DWPF	Without Uncertain & Scaled Runs (WU/WS) (NRH10)	Without Uncertain (WU) (NRH4)	Scaled Runs (SR) (NRH8)	4L	22L	220L	DWPF
Incpt	I	0.9395	1.0027	0.9237				0.9659	0.9736	0.8571				
SASV or HSV	a	0.3410	0.1159	0.0760	0.55	0.1	0.01	0.1279	0.0712	0.0437	1.27	0.37	0.59	0.32
AS	b	0.1423	0.1362	0.2178	105%	105%	105%	0.1421	0.1435	0.2234	105%	105%	105%	105%
PRA	c	-0.8254	-0.6976	-0.6868	55%	55%	55%	-0.8260	-0.7054	-0.5996	55%	55%	55%	55%

WU/WS: without Uncertain *and* Scaled Runs WU: without Uncertain SR: Scaled Runs

Table 3-14 shows the predicted N_R values for the linear models using the input variable values from Table 3-13. The predictions are divided into the contributions from each variable. The 4-L models using SASV and HSV give the same predicted N_R values for each data set. The contribution to the headspace variable is smallest for the SR data that contain the tests at lower SASV and HSV. These results are qualitatively consistent with the observation that there were probably more internal refluxing and more NO_x to nitrate conversion in the 4-L tests than in the larger scale tests.

The predictions for the 22- and 220-L tests are shown in the center of Table 3-14. The contributions from the Intercept, AS, and PRA remain the same at all scales. The contribution of the headspace variables to the predicted N_R value becomes less as expected. The N_R values for the 22- and 220-L runs were lower than the 4-L runs at comparable AS and PRA values, and this is reflected in the predicted values.

The predictions for DWPF, at the same conditions, result in only slightly lower N_R values because the effects of SASV or HSV are relatively small due to their small values. These results suggest that since the headspace variables have relatively small effects on the N_R model, the expected values in DWPF will be similar to those found for the larger scale runs. Overall, the N_R values for the larger-scale tests and DWPF are only about 4-7% lower than for the 4-L runs for these specific values of AS and PRA.

To demonstrate that the models for All Data without Uncertain and the Scaled Runs data have very similar predictions, the predicted values are plotted versus the measured values for the two models for both SASV and HSV in Figures 13 and 14. The Scaled Runs data points have been shown with the symbols ‘4’ for 4-L, ‘M’ for 22-L, and ‘L’ for the 200-L tests. The remaining 4-L test data are shown with the symbols as indicated on the graphs. Fitted lines, representing simple regressions of the predicted values to the measured values, for All Data without Uncertain (black) and the SR data (red) are shown on these plots and these models are very similar, indicating that either model would give approximately the same predictions.

Table 3-14. Contributions of Variables to Predicted N_R for Linear Models

SASV Models				HSV Models			
4L				**4L**			
	WU/WS	**WU**	**SR**		**WU/WS**	**WU**	**SR**
Incpt	94%	100%	92%	Incpt	97%	97%	86%
SASV*Value	19%	6%	4%	HSV*Value	16%	9%	6%
AS*Value	15%	14%	23%	AS*Value	15%	15%	23%
PRA*Value	-45%	-38%	-38%	PRA*Value	-45%	-39%	-33%
Predicted N_R	**82%**	**83%**	**82%**	**Predicted N_R**	**82%**	**83%**	**82%**
				22L			
					WU/WS	**WU**	**SR**
				Incpt	97%	97%	86%
				HSV*Value	5%	3%	2%
22-220L				AS*Value	15%	15%	23%
	WU/WS	**WU**	**SR**	PRA*Value	-45%	-39%	-33%
Incpt	94%	100%	92%	**Predicted N_R**	**71%**	**76%**	**78%**
SASV*Value	3%	1%	1%				
AS*Value	15%	14%	23%	**220L**			
PRA*Value	-45%	-38%	-38%		**WU/WS**	**WU**	**SR**
Predicted N_R	**67%**	**77%**	**78%**	Incpt	97%	97%	86%
				HSV*Value	8%	4%	3%
				AS*Value	15%	15%	23%
				PRA*Value	-45%	-39%	-33%
				Predicted N_R	**74%**	**78%**	**79%**
DWPF				**DWPF**			
	WU/WS	**WU**	**SR**		**WU/WS**	**WU**	**SR**
Incpt	94%	100%	92%	Incpt	97%	97%	86%
SASV*Value	0%	0%	0%	HSV*Value	4%	2%	1%
AS*Value	15%	14%	23%	AS*Value	15%	15%	23%
PRA*Value	-45%	-38%	-38%	PRA*Value	-45%	-39%	-33%
Predicted N_R	**64%**	**76%**	**78%**	**Predicted N_R**	**70%**	**76%**	**78%**

WU: without Uncertain; WU/WS: without Uncertain & without Scaled Runs; SR: Scaled Runs

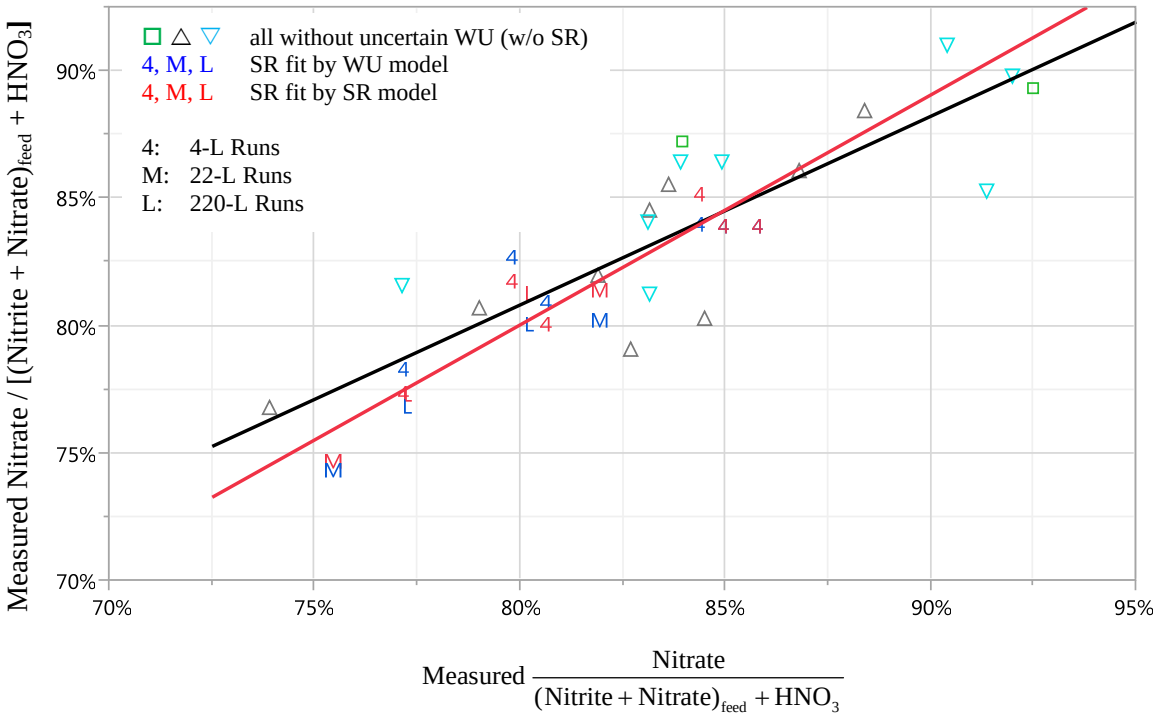

Figure 3-10. Predicted N_R versus SASV for All Data without Uncertain and for Scaled Runs Data

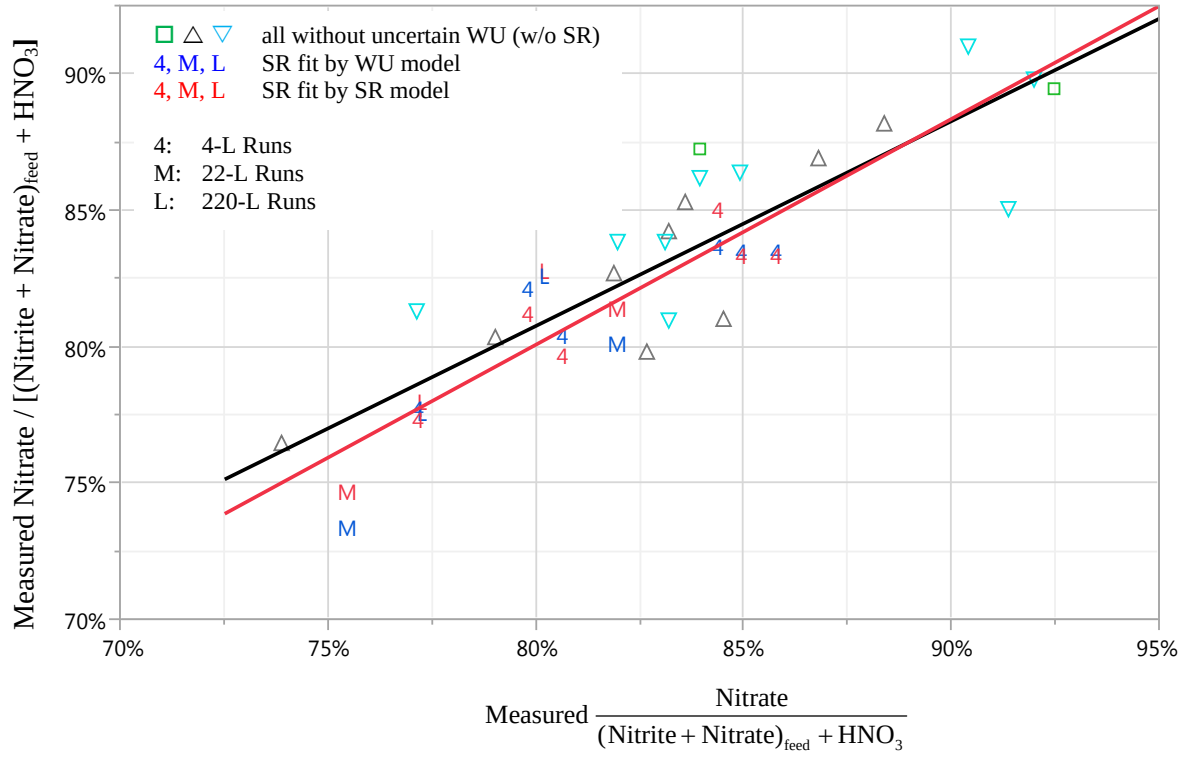

Figure 3-11. Predicted N_R versus HSV for All Data without Uncertain and for Scaled Runs Data

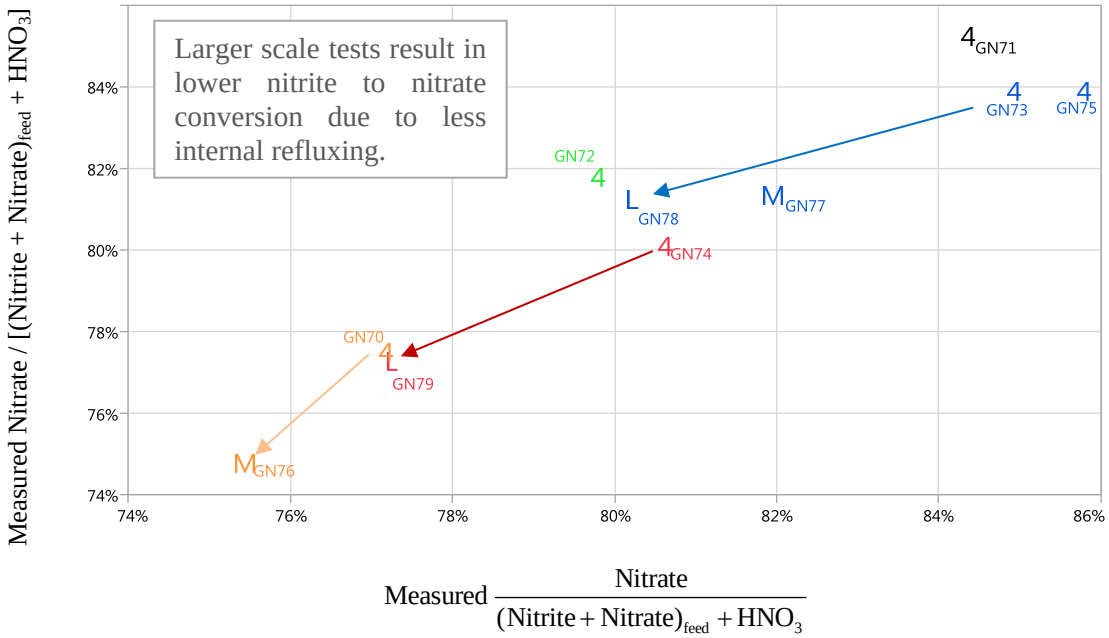

Figure 3-12. Scaled Runs N_R Showing Effect of Scale

3.3 Potential Chemical Reactions of Glycolic Acid and Minimum Acid Requirement

The destruction of glycolic acid in the CPC system by reaction with nitrous or nitric acids, with REDOX metals, or with noble metals is likely to be complex. There are several potential reactions that cannot occur or have been found not to occur and some general observations about the chemistry.

1. Glycolic acid cannot decompose to form two formic acid molecules (REDOX does not balance).
2. Glycolic acid does not appear to disproportionate to formic acid and formaldehyde.
3. Glyoxylic acid does not appear to be formed as an intermediate species (at least not at measurable levels).
4. Without noble metals and mercury present, significantly more formate is found in the products than when noble metals are present. Formate actually accounts for ~30-100% of the glycolic acid destroyed. It has not been determined if it is the absence of the noble metals or mercury or both that result in more formate.

Some potential overall reactions of glycolic acid are shown in Table 3-15. Any reactions with HNO_2 forming NO could also be written with N_2O as the reduced nitrogen species. Reaction [3.10] forming HCOOH and CO_2 is presumed to be the reaction that forms the formate in the absence of noble metals and mercury. Note that a reaction with MnO_2 to give formate could also account for formate generation. Herein, the conversion of glycolate to formate is defined as the extent of this reaction.

Koopman[3] reported that reaction [3.5] is the predominant reaction in the destruction of nitrite in the nitric-formic flowsheet. Any acid can cause this reaction to proceed and it does not involve REDOX reactions of formic acid, and presumably also does not involve REDOX reactions of glycolic acid. Reaction [3.8] is said to account for the N_2O formed from nitrite. Glycolic acid could similarly reduce nitrite to N_2O by reaction [3.9], but three nitrite moles could be reduced per mole of glycolic acid. Koopman states that the direct reduction of nitrite by formic acid by reaction [3.6] only occurs by a noble metals catalyzed pathway; reaction [3.7] for glycolic acid may be similar.

Table 3-15. Reactions of Nitrous Acid, Formic Acid, Glycolic Acid, Manganese, and Mercury

	Nitric-Formic Flowsheet	Nitric-Glycolic Flowsheet
Nitrous Acid Disproportionation	$3\,HNO_2 = HNO_3 + 2\,NO + H_2O$ (Net 2 any acid* required) (75%)†	$3\,HNO_2 = HNO_3 + 2\,NO + H_2O$ [3.5] (Net 2 any acid required)
Nitrous Acid Reduction to NO	$HCO_2H + 2\,HNO_2 = CO_2 + 2\,NO + 2\,H_2O$ [3.6] (2 NO_2^- per formic acid + 2 any acid) (~0%)	$C_2H_4O_3 + 6\,HNO_2 = 2\,CO_2 + 6\,NO + 5\,H_2O$ [3.7] (6 NO_2^- per glycolic acid + 6 any acid)
Nitrous Acid Reduction to N_2O	$HCO_2H + HNO_2 = \frac{1}{2}N_2O + CO_2 + \frac{3}{3}H_2O$ [3.8] (1 NO_2^- per formic acid + 1 any acid) (25%)	$C_2H_4O_3 + 3\,HNO_2 = \frac{3}{2}N_2O + 2\,CO_2 + \frac{7}{2}H_2O$ [3.9] (3 NO_2^- per acid + 3 any acid)
Glycolic Acid to Formic Acid + CO_2	NA	$C_2H_4O_3 + 4\,HNO_2 = HCO_2H + CO_2 + 4\,NO + 3\,H_2O$ [3.10] (4 NO_2^- per acid + 4 any acid)
Glycolic Acid to Oxalic Acid	NA	$C_2H_4O_3 + 4\,HNO_2 = (COOH)_2 + 4\,NO + 3\,H_2O$ [3.11] (4 NO_2^- per acid+ 4 any acid)
Reduction of HgO	$HgO + HCO_2H = Hg^o + CO_2 + H_2O$ [3.12] (1 HgO per formic acid)	$3\,HgO + C_2H_4O_3 = 3\,Hg^o + 2\,CO_2 + 2\,H_2O$ [3.13] (3 HgO per glycolic acid)
Reduction of MnO_2	$MnO_2 + HCO_2H + 2\,H^+ = Mn^{2+} + CO_2 + H_2O$ [3.14] (1 MnO_2 per formic acid + 2 any acid)	$3\,MnO_2 + C_2H_4O_3 + 6\,H^+ = 3\,Mn^{2+} + 2\,CO_2 + 5\,H_2O$ [3.15] (3 MnO_2 per glycolic acid + 6 any acid) $2\,MnO_2 + C_2H_4O_3 + 4\,H^+ = 2\,Mn^{2+} + HCO_2H + CO_2 + 3\,H_2O$ [3.16] (2 MnO_2 per glycolic acid + 4 any acid) $2\,MnO_2 + C_2H_4O_3 + 4\,H^+ = 2\,Mn^{2+} + (COOH)_2 + 3\,H_2O$ [3.17] (2 MnO_2 per glycolic acid + 4 any acid)

* Any acid can supply the H^+ to make HNO_2 from NO_2^-. † Percentage of nitrite by each path (from KMA equation)

The reactions shown in the table show that glycolic acid could be up to three times more reducing than formic acid, so that the amount of glycolic acid required to complete REDOX reactions could be up to three times less than with formic acid. This would mean that for a KMA minimum acid (or similarly an approximately equal Hsu minimum acid) of 100%, the actual acid % acid requirement with the correct stoichiometric equations for glycolic acid would be some value less than 100%.

The Hsu acid requirement[3] as implemented at DWPF was an attempt at a first principles calculation of the *minimum* acid requirement:

$$\frac{\text{moles acid}}{\text{L slurry}} = \left[\text{base equivalents} + 2\times\text{total TIC} + 0.75\times\text{nitrite} + \text{Hg} + 1.2\times\text{Mn})\right] / \text{L} \quad [3.18]$$

Koopman[3] proposed a revised calculation in 2008 based on analysis of more significantly more data for the *minimum* acid requirement (KMA):

$$\frac{\text{moles acid}}{\text{L slurry}} = \left[\text{base equivalents} + \text{Hg} + \text{soluble TIC} + \text{nitrite} + 1.5\times(\text{Ca} + \text{Mg}) + 1.5\times\text{Mn})\right] / \text{L} \quad [3.19]$$

The coefficient on nitrite is an approximate value that would be higher if reduction of nitrite to NO by formic acid (equation [3.6]) occurs to any significant extent.

Koopman also proposed a *nominal* acid requirement based on these additional data that might be a more accurate first principles calculation of the stoichiometric requirement:

$$\frac{\text{moles acid}}{\text{L slurry}} = \left[\text{base equivalents} + \text{Hg} + \text{soluble TIC} + 1.1\times\text{nitrite} + 1.8\times(\text{Ca} + \text{Mg}) + 3\times\text{Mn}\right] / \text{L} \quad [3.20]$$

A revised *minimum* acid requirement (Glycolic Minimum Acid GMA) might be written for glycolic acid based on the reactions in Table 3-15 where the additional reducing power of glycolic acid, less formation of N_2O, and greater reduction of Mn is accounted for in the coefficients on species involved in REDOX reactions:

$$\frac{\text{moles acid}}{\text{L slurry}} = \left[\text{base equivalents} + \frac{\text{Hg}}{3} + \text{soluble TIC} + 0.75\times\text{nitrite} + 1.5\times(\text{Ca} + \text{Mg}) + 0.8\times\text{Mn})\right] / \text{L} \quad [3.21]$$

Using the feed concentrations from Scaled Run GN70, the values of KMA and GMA for several acid stoichiometries are compared in Table 3-16. A KMA acid stoichiometry of 85% is approximately 102% for the proposed actual reactions of glycolic acid as quantified in equation [3.21].

Table 3-16. Comparison of KMA and GMA Acid Stoichiometry Values

KMA Acid Stoichiometry (%)	GMA Acid Stoichiometry (%)
85	102
100	121
125	151

The reactions of nitrite to form N_2O ([3.8]) and of HgO ([3.12]) and MnO_2 ([3.14]) with formic acid all convert one mole per one mole of formic acid in a two-electron transfer. Glycolic acid, with six electrons available, can theoretically convert three moles per mole of acid for each of these reactions ([3.9]- [3.13], [3.15]-[3.17]). Reactions for HgO reduction similar to [3.16] and [3.17] that generate formate and oxalate could also be written (but are not shown in the table).

The results with noble metals and mercury present, where there is little formation of formate or oxalate, show that the complete reaction of glycolic acid with the oxidizing species to form CO_2 occurs overall. What is not apparent from the available data is what intermediate species exist in the oxidation of glycolic acid to CO_2. In the absence of noble metals and mercury, significant formate is generated (e.g., [3.16]) indicating that one or more of the noble metals or mercury appear to be required to completely convert formate to CO_2. As noted in Section 3.5.1, the conversion of glycolate to formate in the absence of noble metals was found to be ~40-100% at 100% acid stoichiometry.

The data to date are insufficient to determine whether formic acid or formate are formed as a stable intermediate (e.g., [3.16]) in the presence of noble metals and mercury, or if there is possibly an unstable reactive intermediate that is converted to CO_2 and H_2O rather than to CO_2 and H_2. In the presence of noble metals and mercury, a hypothetical reaction scheme for MnO_2 reduction might be:

$$2\ MnO_2 + C_2H_4O_3 + 4\ H^+ = 2\ Mn^{2+} + HCO_2H + CO_2 + 3\ H_2O \quad ([3.16])$$

$$HCO_2H + \text{oxidant} \xrightarrow{\text{noble metals}} CO_2 + H_2O$$

The oxidant could be MnO_2, HgO, nitrite, or dissolved O_2. It is not evident at this time why noble metals might be required to further oxidize the formic acid formed and the mechanism of how such an oxidation would be catalyzed. Note that in the Rh catalyzed destruction of formic acid to make CO_2 and H_2, carbon is oxidized from +2 to +4 while two hydrogens are reduced from +1 to zero; an additional oxidant is needed to oxidize H_2 to H_2O.

3.4 Modeling Glycolate Destruction

Glycolate destruction was modeled using the same variables and models used for the nitrite to nitrate conversion. The glycolate destruction was calculated by two methods. The first method used the Ion Chromatography (IC) data for glycolate in the calculations. The second method determined the glycolate destruction from the amount added and the amount of CO_2 generated during acid addition. These two glycolate destruction values were calculated as:

- Glycolate Destruction = Glycolate Added as Glycolic Acid – Glycolate Measured in Product by IC
- Glycolate Destruction = Glycolate Added as Glycolic Acid – (CO_2 Generated – CO_2 from Carbonate)

The CO_2 from carbonate was calculated from the Total Inorganic Carbon (TIC) content of the feed sludge. In several cases, the actual carbonate added in producing the sludge was used rather than the measured TIC value because the measured value was deemed to be less accurate.

The fits of glycolate destruction from IC data versus the variables for the All Data, All Data without Uncertain, and the Scaled Runs are shown in Table 3-17. As was the case with the nitrite to nitrate conversion, the All Data fit was poor; adding several quadratic terms improved the fit significantly, but it is difficult to justify the cross terms found to be significant. Using the corrected variables resulted in even lower R^2 values for the All Data set. The only consistent variable was the need for the Acid Stoichiometry in the models.

Table 3-17. Fit of Glycolate Destruction from IC Analyses to SASV and HSV and Additional Parameters

Data Set:		All Data			Without Uncertain						
Identifier:		GdIC1	GdIC2	GdIC3	GdIC4a	GdIC5	GdIC6	GdIC7	GdIC8	GdIC9	GdIC10
R^2		0.39	0.67	0.67	0.88	0.81	0.80	0.76	0.73	0.96	0.90
R^2 adjusted		0.34	0.59	0.59	0.84	0.77	0.76	0.72	0.69	0.93	0.85
					Without HSV						Allow both SASV & HSV
Surface Area/Sludge Volume	(SASV)										
Headspace Volume/Sludge Volume	(HSV)										
Acid Stoichiometry	(AS)										
Percent Reducing Acid	(PRA)										
Noble Metals Present	(NM)										
Nitrite (initial)											
Nitrate (initial)											
Oxalate (initial)											
Mn											
Fe											
Nonlinear (Quadratic) Terms			oxalate*Mn	$nitrite^2$						$SASV^2$	
			AS*Fe	AS*Fe						SASV*AS	
			PRA*Fe	nitrite*Fe						SASV*NM	
				nitrate*Fe						SASV*PRA	
										$nitrate^2$	
										AS*oxalate	
										nitrate*Fe	

Data Set:		Without Uncertain						Scaled Runs		
Identifier:		GdIC11a	GdIC12a	GdIC13	GdIC14	GdIC15	GdIC16	GdIC17	GdIC18	GdIC19
R^2		0.88	0.83	0.84	0.76	0.73	0.97	0.78	0.84	0.91
R^2 adjusted		0.84	0.79	0.79	0.72	0.69	0.94	0.75	0.72	0.84
		Without SASV								
				With NM						
Surface Area/Sludge Volume	(SASV)								see	
Headspace Volume/Sludge Volume	(HSV)								below	
Acid Stoichiometry	(AS)									
Percent Reducing Acid	(PRA)									
Noble Metals Present	(NM)									
Nitrite (initial)										
Nitrate (initial)										
Oxalate (initial)										
Mn										
Fe										
Nonlinear (Quadratic) Terms							HSV*AS			HSV^2
							HSV*PRA			HSV*AS
							HSV*NM			
							PRA*NM	Note: Prob > |t|		
							$nitrate^2$	**>0.2, <0.3**		
							HSV*oxalate	not significant, but included		
							AS*oxalate			

Note GdIC4a and GdIC11a are identical

3.4.1 Glycolate Destruction Fit Without HSV

The Without Uncertain data were fit without HSV to various sets of the variables as shown in columns GdIC4a-8. In no cases except the quadratic (GdIC9) was SASV found to be significant. PRA was slightly to marginally significant. In GdIC4a with all possible linear variables, nitrite, nitrate, oxalate, Mn and Fe were found to be significant. Since Mn and Fe are correlated, Mn was removed, but the resulting fit of the data had a smaller R^2.

Removing nitrite from consideration resulted in nitrate no longer being significant but NM now was significant. Overall, it appears that for the WU data the variables AS, PRA, and Fe are needed, and

oxalate and nitrate help improve the fit slightly; having both nitrite and nitrate and both Mn and Fe surprisingly improves the fit even more. The inconsistency of the presence of nitrate and noble metals suggests these are not really important variables (at least for the data available). Oxalate does appear to be possibly important. The importance of oxalate might make some sense chemically. Oxalate is known to be one of the products of glycolate decomposition, so an effect on the decomposition is not out of the question.

The JMP linear fits for All Data and without Uncertain data (fit GdIC6) are shown in Figure 3-13. As was the case with nitrite to nitrate, the variation in the glycolate destruction values for the Uncertain data cannot be modeled effectively by the known variables. The yellow highlights, on the left graphic for Figure 13, show that there are actually only two predicted values between 17-18% whereas the measured data range from 10-31%. As shown in the right graphic for Figure 13, the fit of the data without Uncertain is significantly better.

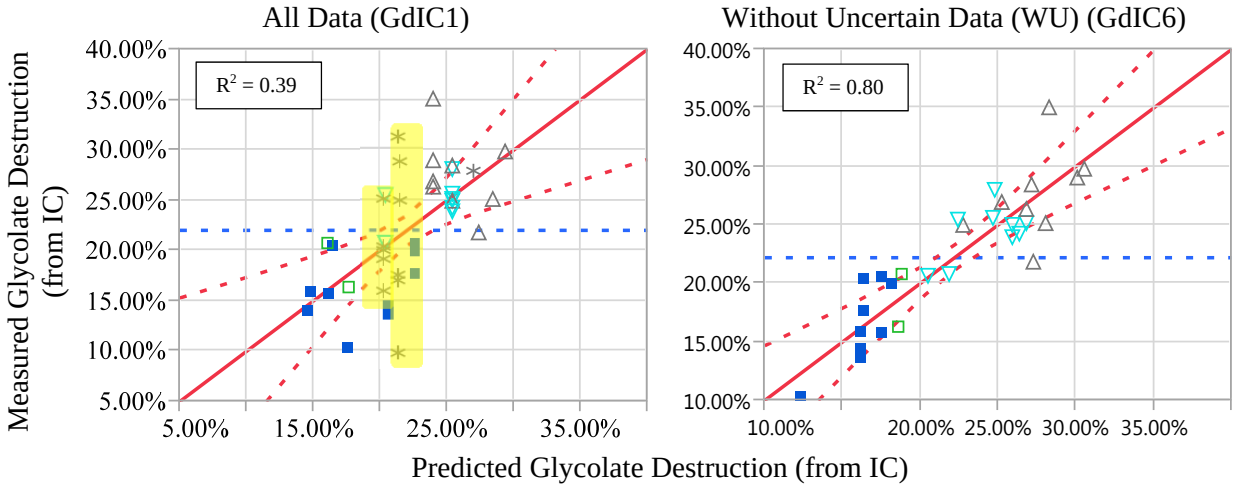

Figure 3-13. Comparison of Glycolate Decomposition Fits

3.4.2 Glycolate Destruction Fit With HSV

Similar results were found when fitting using the HSV variable, except that HSV was found to be at least marginally significant in more of the models. Acid Stoichiometry is again significant, and Percent Reducing Acid is again somewhat significant. The GdIC11a is identical to the GdIC4a fit. The GdIC12 fit shows the fit is slightly less good when Mn and nitrite are removed, and GdIC13 shows the fit with the no noble metals data also removed. This latter fit is almost exactly the same as with the no noble metals data present except nitrate became insignificant. Removing Mn, oxalate, and nitrite reduce the R^2 more as shown in GdIC14-15. In GdIC10, both HSV and SASV were allowed to be in the model; including both gave the highest R^2 with only linear variables, but all variables except NM were significant. The most significant variables across the models for fitting versus HSV are AS, PRA, and Fe. Oxalate appears to possibly be important, and also possibly nitrate or nitrite.

In the fit of just the Scaled Runs data, the only significant variable was acid stoichiometry (GdIC17). When the model was allowed to retain all variables regardless of significance, the R^2 improved from 0.78 to 0.84 but the adjusted R^2 decreased. The quadratic fit improved R^2 to 0.91. These three fits are shown in Figure 3-14. The fit versus AS only has only three predicted values since there were only three acid stoichiometries run. The addition of the insignificant variables results in more predicted values, but note that the 95% confidence bands are actually larger (as reflected by the lower adjusted R^2).

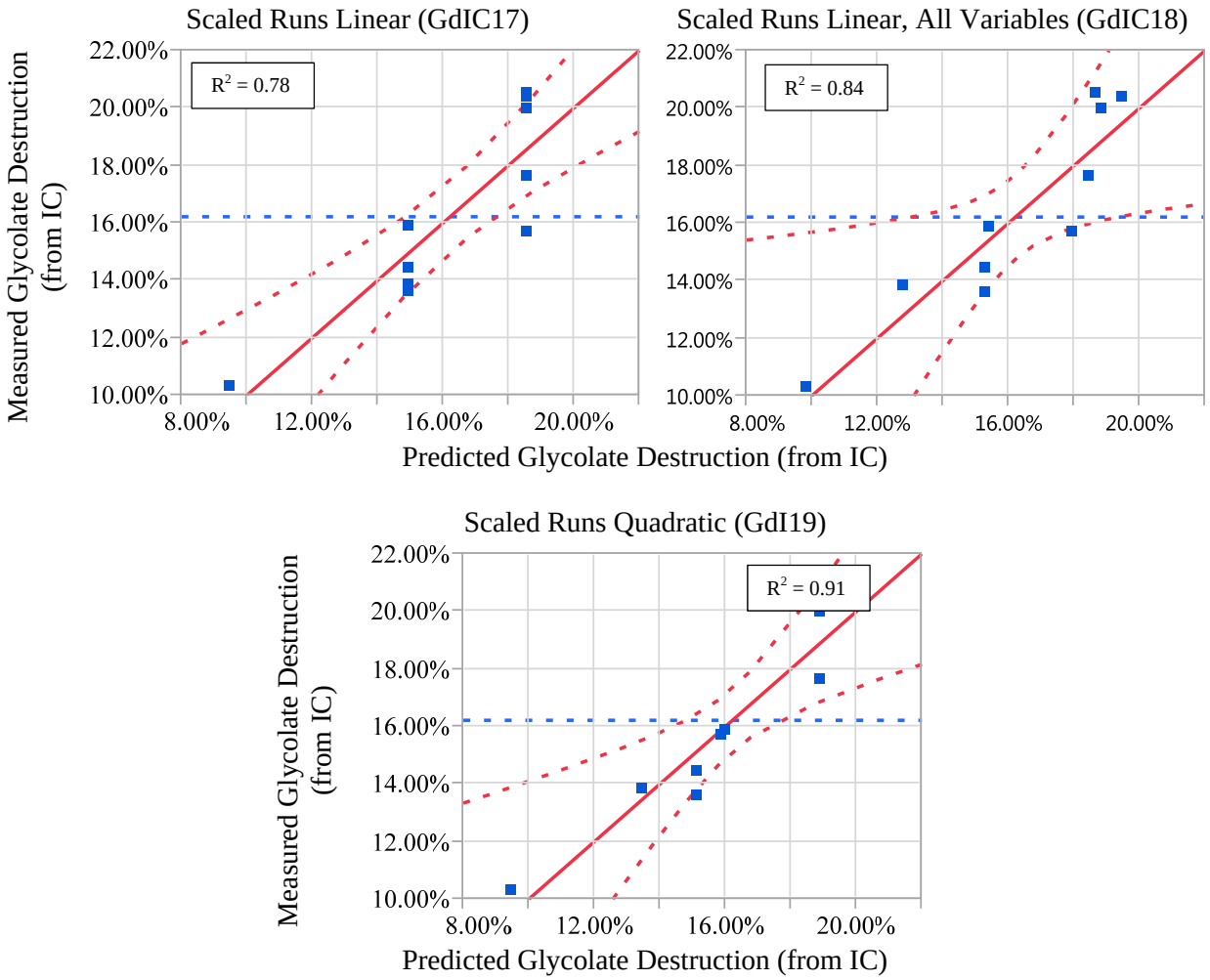

Figure 3-14. Comparison of Glycolate Decomposition from IC Data Fits

The fits of the glycolate destruction from IC data are not nearly as good as the fits of the N_R data. There is significant variation that cannot be accounted for by the proposed variables. Note that if there is any dependence of the glycolate destruction on the nitrite chemistry, this dependence would be absorbed by the models since the models for both glycolate destruction and nitrite to nitrate conversion have the same variables.

Another way to look at the fits of the data is to compare the predicted values from the models for specific data sets or variables. Predicted values for several data sets are shown in Table 3-18. The ±5% and ±10% regions around each measured value are shown highlighted in green and yellow, respectively. Note that there is no single model that predicts all of the measured values within 10%. The best fitting model (of those shown here) is the quadratic model with no headspace dependence. The best linear model is GdIC4a or 11a; GdIC5 or 12 are reasonable models containing less variables but still having relatively high R^2 values.

Table 3-18. Fit of Several Experimental Data Sets Glycolate Destruction by Models

				Headspace Term:			SASV	None					
					Data Set:		ALL	Without Uncertain (WU)					
				Number of Variables:			3	5	5	5	4	4	Quadratic
	Model	lo	hi	lo	hi	R^2:	0.39	0.81	0.81	0.80	0.76	0.73	0.96
Run	Measured	10%	10%	5%	5%	GdIC:	1	4	5	6	7	8	9
GN40	**16.3%**	14.7%	18.0%	15.5%	17.1%		17.7%	16.5%	17.2%	18.6%	22.3%	21.6%	16.3%
GN48	**27.0%**	24.3%	29.6%	25.6%	28.3%		23.9%	25.4%	25.4%	25.2%	24.6%	23.2%	25.8%
GN50	**29.0%**	26.1%	31.9%	27.6%	30.5%		23.9%	29.7%	29.6%	30.1%	28.6%	28.7%	29.4%
GN70	**17.6%**	15.8%	19.4%	16.7%	18.5%		22.6%	16.3%	16.3%	16.4%	17.2%	17.5%	19.1%
GN71	**10.3%**	9.6%	11.8%	10.2%	11.2%		17.6%	12.6%	12.5%	12.4%	11.6%	10.6%	9.5%
GN77	**15.9%**	14.3%	17.5%	15.1%	16.7%		14.9%	16.1%	16.0%	16.2%	16.1%	16.3%	14.9%
GN79	**15.7%**	14.1%	17.3%	14.9%	16.5%		16.2%	17.3%	17.3%	17.5%	18.1%	18.7%	15.1%

				Headspace Term:			HSV			None	Both
					Data Set:		WU	Without (Unc. & NM)	WU	Scaled Runs	
				Number of Variables:			6	5	8	1	4
	Model	lo	hi	lo	hi	R^2:	0.83	0.84	0.88	0.78	0.84
Run	Measured	10%	10%	5%	5%	GdIC:	12	13	11	17	18
GN40	**16.3%**	14.7%	18.0%	15.5%	17.1%		16.8%	18.5%	16.1%	7.7%	7.3%
GN48	**27.0%**	24.3%	29.6%	25.6%	28.3%		26.4%	25.3%	25.6%	18.6%	17.7%
GN50	**29.0%**	26.1%	31.9%	27.6%	30.5%		30.7%	31.7%	28.5%	18.6%	18.6%
GN70	**17.6%**	15.8%	19.4%	16.7%	18.5%		15.5%	15.7%	16.0%	18.6%	18.5%
GN71	**10.3%**	9.6%	11.8%	10.2%	11.2%		11.7%	10.1%	11.9%	9.5%	9.9%
GN77	**15.9%**	14.3%	17.5%	15.1%	16.7%		17.7%	17.7%	16.8%	14.9%	15.4%
GN79	**15.7%**	14.1%	17.3%	14.9%	16.5%		18.6%	19.2%	16.0%	18.6%	17.9%

Green: within ±5%; Yellow: within ±10%.; blue values indicate model not valid for these runs

3.4.3 Glycolate Destruction from Offgas Data

In Figure 3-15, it is apparent that the range of the data for each data type is very different. The Scaled Runs and runs 40-41 data are all below 21%, the no noble metals data are between 20-28%, and the remaining data with noble metals is all above 24% except for one point. The measured glycolate destruction values are shown by data type in Figure 3-15. The glycolate destruction from the offgas data is also shown. There are only 17 data points for the offgas; 10 are the Scaled Runs and 7 are from the other runs (3 from Uncertain, 1 from GN40, three from the GN43-50 series).

The glycolate destructions calculated from the offgas data are smaller than the corresponding values from the IC data for all but two data points. A plot of these data is shown in Figure 3-16. The dotted black line is the y=x line that the data would be expected to lie on. The blue line is a linear fit of the SR data. The 95% confidence interval almost encompasses the y=x line, but most of the data points are below this line. The higher values from the IC data for the older samples may indicate that there is degradation of the samples upon storage for extended periods of time; this possibility is noted in Section 3.5.2 for the glycolate to oxalate conversion. However, glycolate decomposition probably does not account for the lower values for the Scaled Runs because these samples were not very old when analyzed.

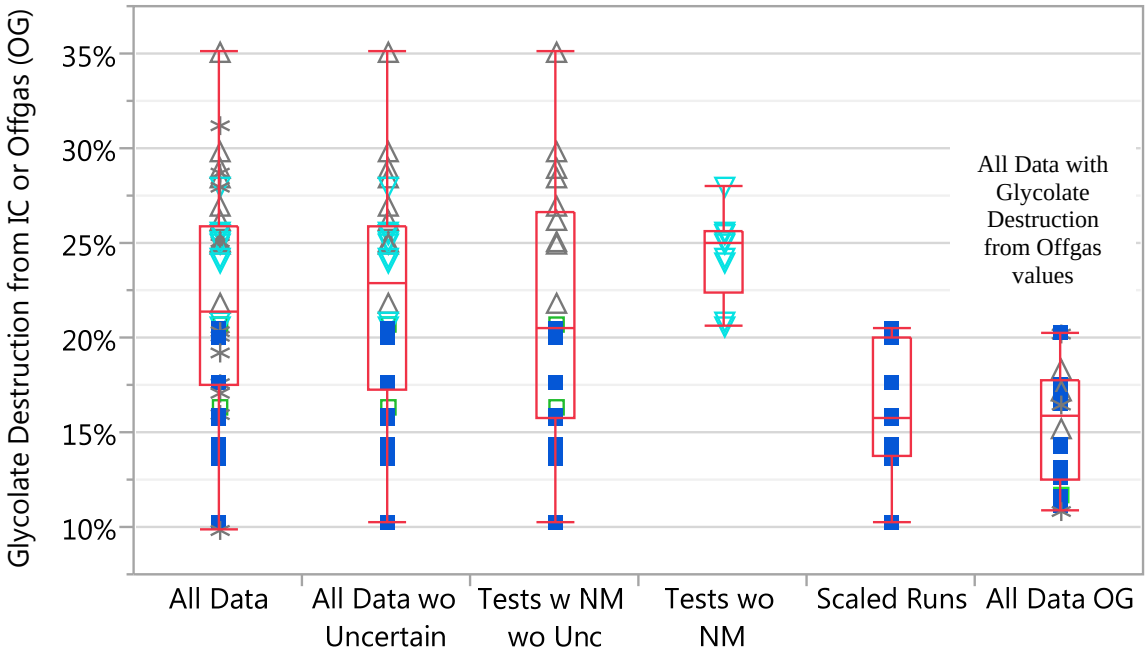

Figure 3-15. Glycolate Destruction by Model Grouping

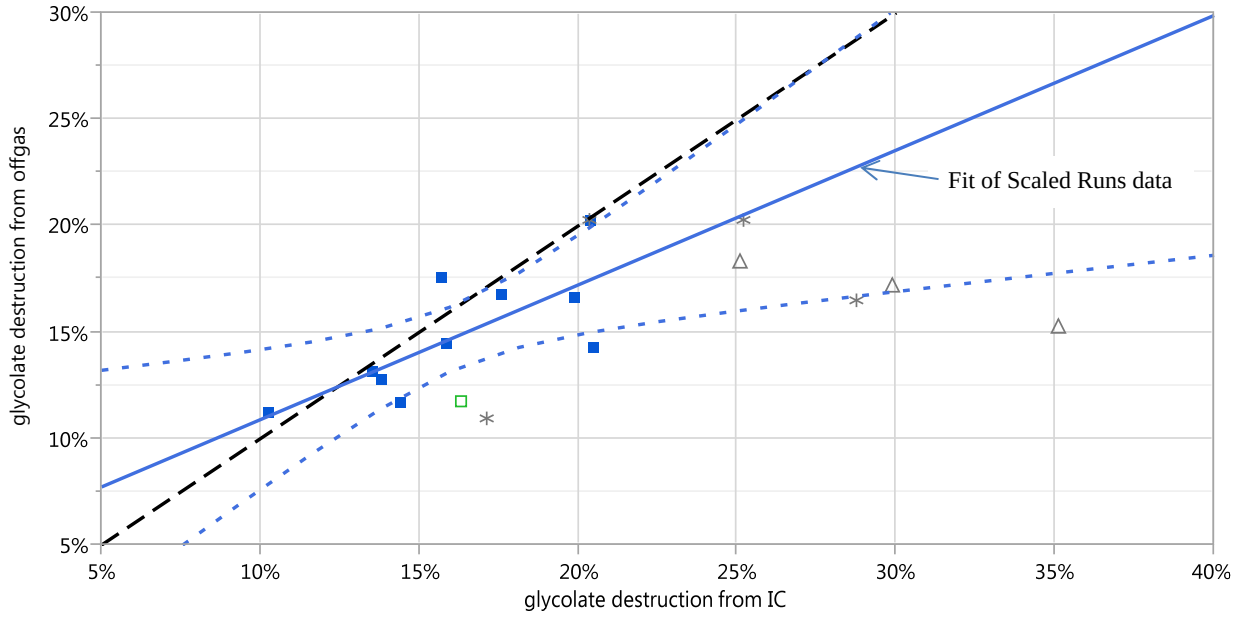

Figure 3-16. Glycolate Destruction from Offgas versus from IC Data

The best linear fits of the glycolate destruction from offgas data are shown in Figure 3-17. The All Data model has the variables AS, oxalate, and Fe significant and no dependence on headspace. The Scaled Runs data in the figure then have only three predicted values since oxalate and Fe were not varied. The fit improves significantly when the Uncertain data points (3) are removed. With the Uncertain data removed,

the significant variables are HSV, AS, PRA, and Fe so the prediction of the SR data is greatly improved. Adding HSV and PRA to the All Data model only improves R^2 from 0.64 to 0.66.

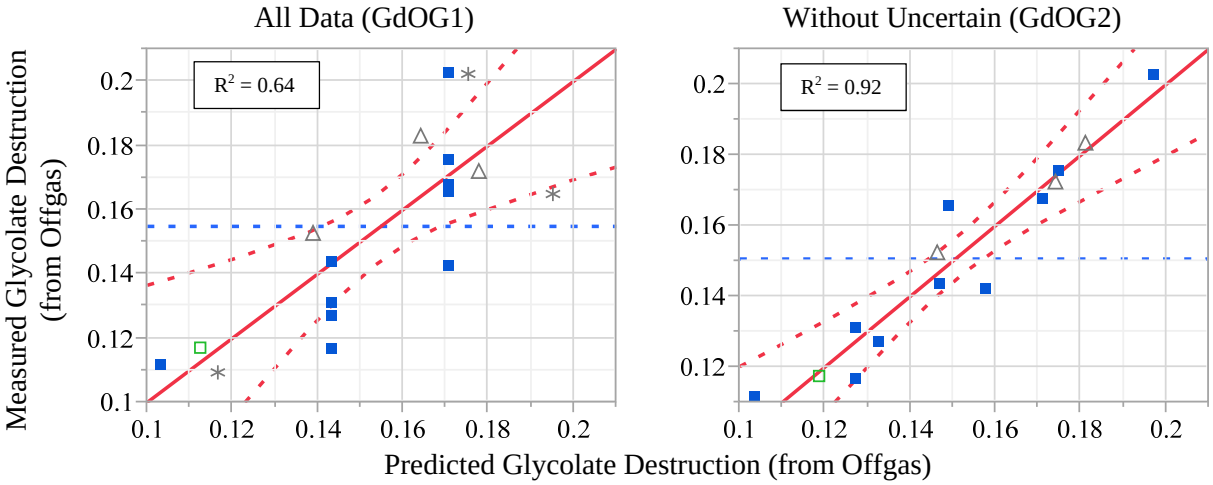

Figure 3-17. Comparison of Glycolate Decomposition from Offgas Data Fits

The glycolate destruction by IC data has significantly greater scatter than the data from the offgas measurements. Several reasons for this greater scatter are that there are just more IC data, that much of the IC data is from older less reliable IC data or from caustic quench IC data performed on old samples, and that the SR tests done with offgas analysis were done more carefully and rigorously (many of the earlier tests were scoping tests that did not have the specific purpose of performing accurate carbon balances).

3.5 Glycolate Conversion to Formate + CO_2 and to Oxalate

3.5.1 Glycolate Conversion to Formate + CO_2

The conversion of glycolate to formate + CO_2 (per reaction equation [3.10]) is small with noble metals and mercury present, but significantly larger when these are missing. Figure 3-18 shows these data for the All Data, All Data without noble metals, and All Data with noble metals. These graphs show that with noble metals present, the conversion to formate is under 3% and cannot be correlated for the All Data set. This conversion is so low that it should just be assumed to be about 1% for all tests with noble metals and mercury present.

For the tests without noble metals and mercury, the conversion to formate can be correlated with acid stoichiometry and weakly with SASV as shown in Figure 3-18. The runs without NM or Hg did not vary any of the other variables except PRA, which was not found to be significant. The All Data plot shows that all of the data correlation is essentially due to the data without NM and Hg.

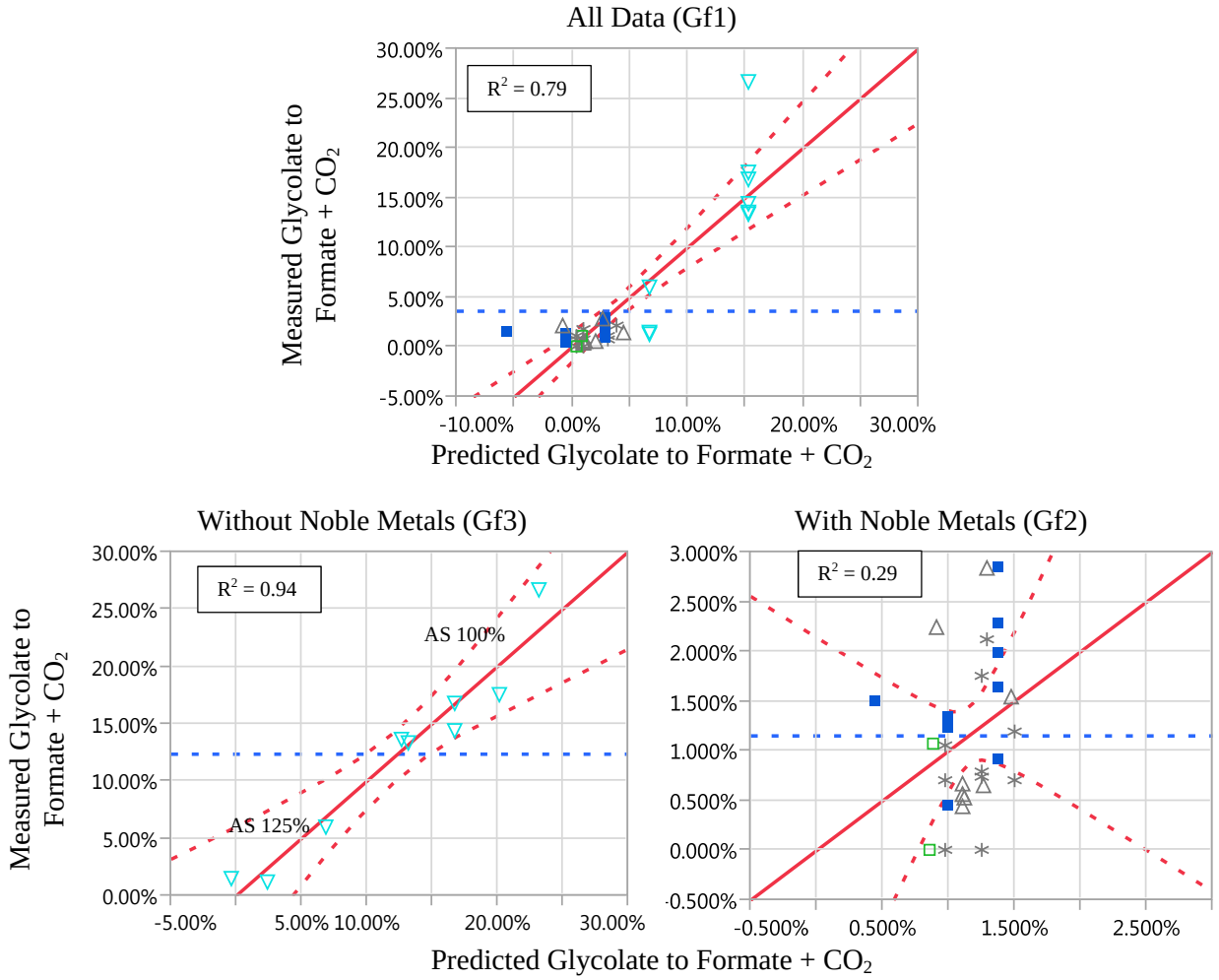

Figure 3-18. Comparison of Glycolate Conversion to Formate and CO_2 Fits

These results show that minimal formate is formed when noble metals and Hg are present. High acid stoichiometry (125%) without NM and Hg also results in low formation of formate. The glycolate to formate data are shown by grouping in Figure 3-19. The Scaled Runs, Uncertain, and other with NM data are approximately equal. The no NM data at 125% acid are similar with one point being higher than 5%. The data for no NM at 100% AS have a mean of about 17%.

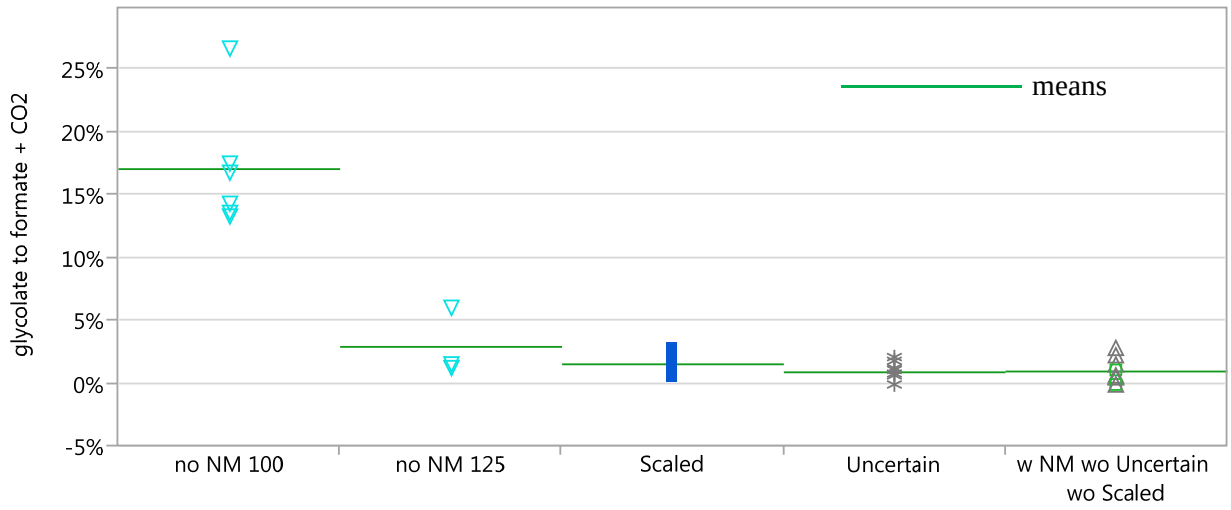

Figure 3-19. Glycolate to Formate + CO_2 by Grouping

At 100% acid stoichiometry and no noble metals, the conversion of glycolate to formate relative to total glycolate destruction decreased as the percentage of reducing acid (glycolic acid) was increased. In other words, adding more glycolic acid relative to nitric acid resulted in higher relative conversion to formate and CO_2 versus to only CO_2. These results are shown graphically in Figure 3-20. The 125% acid stoichiometry data show the opposite relationship, but there are only 3 data points, so it is difficult to draw conclusions.

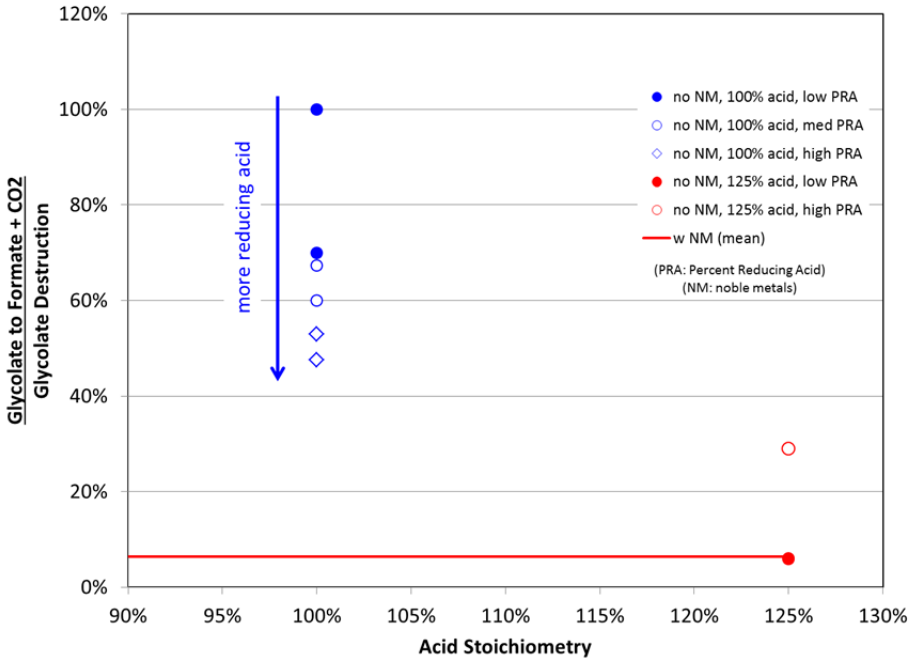

Figure 3-20. Glycolate to Formate Ratio to Glycolate Destruction versus Acid Stoichiometry

It appears that the overall effect of high acid is similar to the effect of noble metals and Hg. These results imply that without noble metals and Hg, formate and CO_2 are formed from the decomposition of glycolate. With NM and Hg, the formate is either not formed or if formed, it is destroyed and does not end up in the products. It would appear that the noble metals or Hg is involved in the destruction of intermediately generated formate or is causing a different reaction path that does not generate formate.

For the no noble metals and Hg with high acid data, there must be a different reaction path occurring that does not generate formate since it does not seem likely that formate would be destroyed without the presence of NM and Hg.

It is also illuminating to look at the glycolate to formate + CO_2 ratio to the glycolate destruction, as shown in Figure 3-21. This value indicates how much of the glycolate destroyed was converted to formate + CO_2 rather than completely to CO_2 or to oxalate. The bottom graph shows this ratio for all data with noble metals. Even though the percentage of total glycolate fed that is converted to formate is less than 3%, the fraction that this formate is of the glycolate destroyed is surprisingly high. Up to 15% of the glycolate destroyed in the presence of noble metals and Hg results in formate + CO_2. Without noble metals present and at 100% acid stoichiometry, this percentage was 42-100%, with most values around 60%.

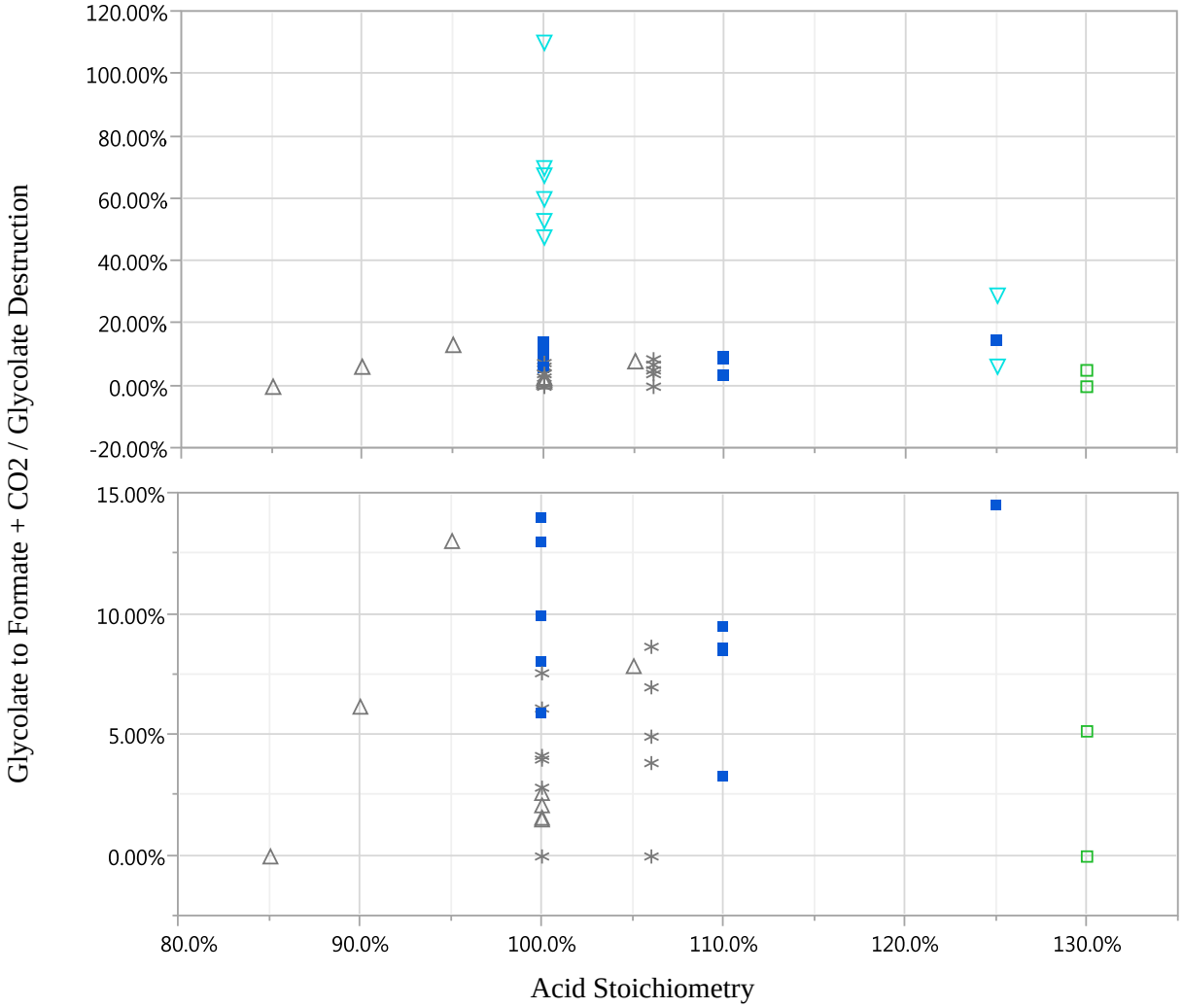

Figure 3-21. Ratio of Glycolate to Formate + CO_2 to Glycolate Destruction

3.5.2 Glycolate Conversion to Oxalate

The glycolate conversion to oxalate data are inconclusive. Most of the oxalate concentration data used were from re-analyses of old samples using the recently developed caustic quench IC method. This method results in higher oxalate concentrations in SRAT and SME products that are believed to be more

accurate than the results from water-only dilution. However, it appears that upon storage, glycolate in SRAT or SME samples may decompose to oxalate. This decomposition would not affect the calculated glycolate destruction value too much, but could result in much higher glycolate to oxalate values. The glycolate to oxalate conversions by data group are shown in Figure 3-22. The age of the samples from left to right is newest to oldest. The graph distinctly shows that older samples have higher oxalate conversions.

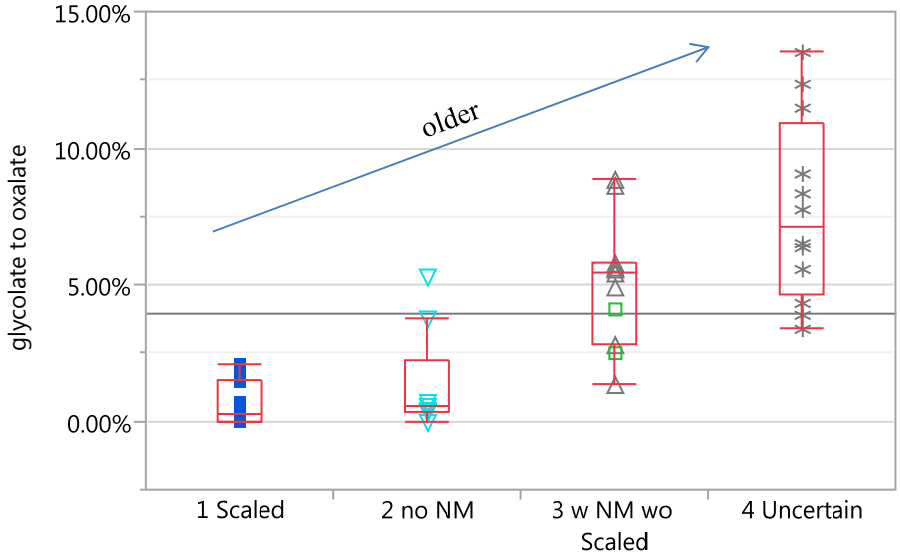

Figure 3-22. Glycolate to Oxalate Conversion by Grouping

Even though it appears that the conversion to oxalate may be due to aging, it was possible to fit the conversion reasonably well to a function of HSV, acid stoichiometry, nitrate, Mn and Fe with an R^2 of 0.62. It is recommended that a glycolate to oxalate conversion value of about 1-2% be used until additional data can be collected.

3.6 Propagation of Error from Models to the REDOX Equation

The intent of the models is to be able to predict the composition of the SRAT or SME product from the sludge feed composition and a pair of acid stoichiometry and percent reducing acid values (and a specific equipment headspace variable). The variation in the experimental data that went into the model results in uncertainty in the predicted values for the compositions. The uncertainty in the predicted composition values can be propagated into the REDOX equation to estimate the uncertainty in the resulting glass REDOX (assuming there is no error in the REDOX model). Tables 17 and 21 gave some approximations to the uncertainty in the N_R nitrite to nitrate conversion and the glycolate destruction from IC values. More statistically rigorous uncertainty values are described below.

The uncertainties in the mean measured value and an individual measured outcome for glycolate destruction are shown in Figure 3-23. The model used for this example (GdIC12) was linear and included HSV, AS, PRA, nitrate, oxalate and Fe. The fitted line is shown in solid red. There are two confidence intervals shown. The orange (inner) lines are the 95% confidence interval on the mean, and the blue (outer) lines are for a single, individual outcome. For example, for a predicted value of about 20%, the 95% confidence interval on mean value is about 16-23%. The confidence interval on an individual outcome is larger at about 13-26%. These intervals are larger than the ±10% intervals given in Table 3-18. The confidence interval on an individual point means that there is 95% confidence that any given data point will be within this interval. The confidence interval on the mean value is smaller because it is the confidence that the average value from several tests will be within this interval. Also, note that most of the experimental data fall within the confidence interval for individual values.

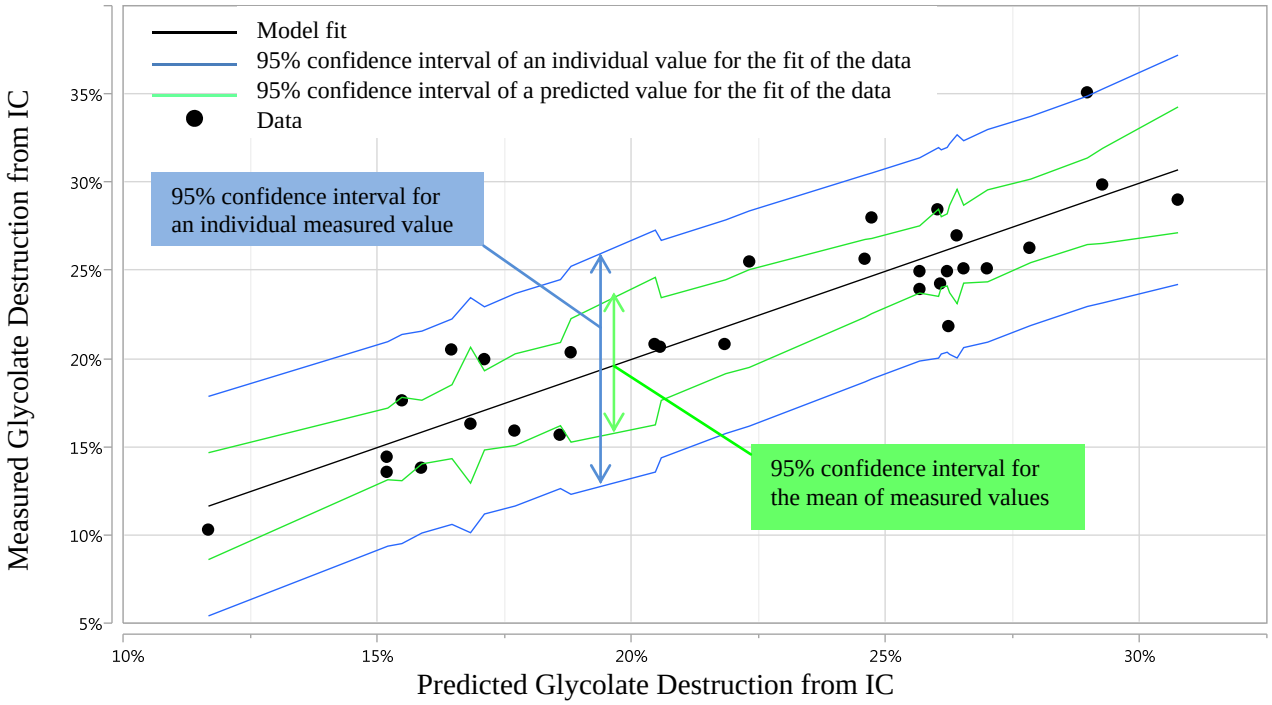

Figure 3-23. Uncertainty in Glycolate Destruction

A similar plot is shown for the nitrite to nitrate conversion N_R data in Figure 3-24. Here the confidence intervals on the fitted mean and an individual data point at a N_R value of about 85% are 83.5-87.5% and 79.5-91%, respectively.

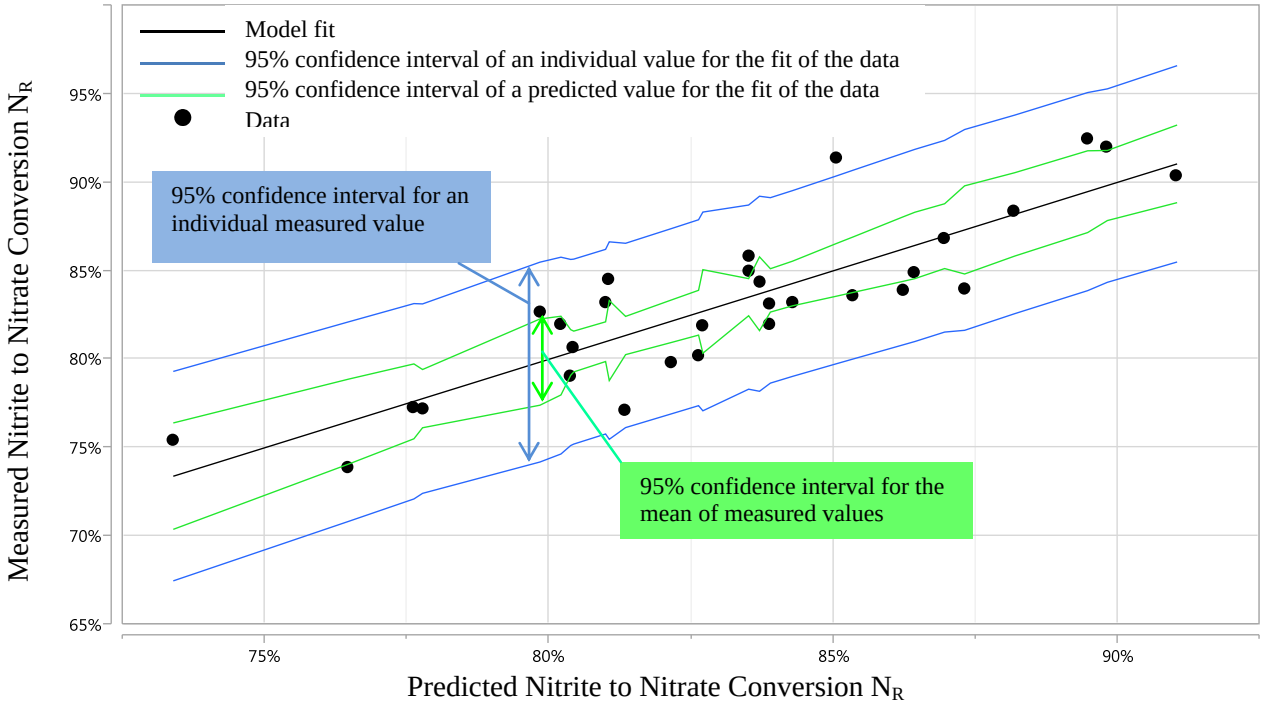

Figure 3-24. Uncertainty in Nitrite to Nitrate Conversion N_R

Using these approximate error bounds, the predicted REDOX values were calculated for a hypothetical case (actually Scaled Run GN70). The input data for these calculations are shown in Table 3-19. The nitrite to nitrate conversion N_R was calculated from the linear model with HSV, AS, and PRA (NRH4); the glycolate destruction was calculated from the linear model with HSV, AS, PRA, nitrate, oxalate, and Fe (GdIC13). The 'Range' for the conversions is the lower and higher values used to calculate the range of predicted REDOX values. The range values are from the individual confidence intervals as described in Figures 26–27. The SME compositions were calculated from the anion concentration data from the GN70 acid calculation sheet.

The REDOX values for the predicted conversion values and the low and high estimates are shown in Table 3-20. The REDOX equation used was:

$$\frac{Fe^{2+}}{\sum Fe} = 0.2358 + 0.1999\left(2[F] + 4[C] + 4[O_T] + 6[G] + 2.88[A] - 5[N] - 2[Mn]\right)\frac{45}{T}$$

where [F] = formate (mol/kg feed)
[C] = coal (carbon) (mol/kg feed)
[O_T] = $oxalate_{total}$ (soluble and insoluble) (mol/kg feed)
[G] = glycolate (mol/kg feed)
[N] = nitrate + nitrite (mol/kg feed)
[Mn] = manganese (mol/kg feed)
T = total solids (wt%)

High destruction and high nitrite to nitrate conversion give the lowest estimated REDOX, whereas low glycolate destruction and low nitrite to nitrate conversion give the highest estimated REDOX. This example shows that the uncertainty (approximate 95% confidence intervals on individual values) on the predicted REDOX value of 0.117 is from 0 to 0.214. The adequacy of the REDOX model (SME compositions to predicted REDOX) is not included in this analysis.

Table 3-19. Inputs to Calculating Uncertainty in REDOX from Predicted Conversions for GN70 Data

Sludge Composition			
Total Solids	wt%	17.5	
Calcine Solids (CS)	wt%	12.7	
Nitrite	mg/kg	12365	
Nitrate	mg/kg	8102	
Oxalate	mg/kg	2013	
Formate	mg/kg	0	
Antifoam	mol/kg in SME	0.04	
Mn	wt% CS	7.59	
Fe	wt% CS	24.4	
Acid Calculations		**Assumed (Range)**	**Actual**
Acid Stoichiometry	%	100	
Percent Reducing Acid	%	58.31	
Nitrite to Nitrate Conversion NR	%	77.78 (72.42-83.13)	77.18
Glycolate Destruction	%	15.47 (9.55-21.40)	17.60
Glycolate to Formate	%	1.0	2.3
Glycolate to Oxalate	%	2.0	1.5
SME Total Solids	wt%	49.3	
Target Waste Loading	%	36	
REDOX Equation			
Glycolate Coefficient	6		
Nitrate Coefficient	5		
Mn Coefficient	5		

Table 3-20. Uncertainties in Predicted REDOX Values

	REDOX
Glycolate Destruction High, Nitrite to Nitrate Conversion High	0
Glycolate Destruction High, Nitrite to Nitrate Conversion Low	0.104
Predicted REDOX	**0.106**
REDOX from measured conversions	**0.092**
REDOX from measured SME composition	**0.089**
Glycolate Destruction Low, Nitrite to Nitrate Conversion High	0.107
Glycolate Destruction Low, Nitrite to Nitrate Conversion Low	0.214

3.7 Implementation of Predictive Models

The implementation of these models into the Acid Calculation spreadsheet for simulant testing will require several modifications. Currently, the Percent Reducing Acid required is calculated to make the predicted REDOX match the target value. Other than the composition of the sludge, the additional inputs needed are:

1. Percent Reducing Acid
2. Nitrite to nitrate conversion
3. Glycolate destruction
4. Glycolate to formate conversion
5. Glycolate to oxalate conversion

The glycolate to formate conversion (with noble metals and mercury) should be assumed to be about 1% (0-2%) and can be changed based on specific experience with a particular sludge batch. If noble metals and mercury are not present, the model for glycolate conversion to formate Gf3 (Figure 3-18) should be used. The glycolate to oxalate conversion should be assumed to be about 2% until additional data can be added to the models to refine the fit. The recommended models for estimating these quantities are given in Table 3-21. For glycolate destruction, either the more general model including sludge composition variables or the more specific model for the Scaled Runs (SB8 sludge) could be used.

Table 3-21. Recommended Equations for Predicting Conversions

Quantity Predicted	**Equation**						
Nitrite to Nitrate Conversion N_R	$N_R = I + a(HSV) + b(AS) + c(PRA)$ $R^2 = 0.74$ (NRH4a)						
Coefficients	I	a	b	c			
	0.9615	0.09068	0.1397	-0.6994			
Glycolate Destruction (multiple sludges)	Glycolate Destruction $= I + a(HSV) + b(AS) + c(PRA) + d(\text{nitrate}) + e(\text{oxalate}) + f(Fe)$ $R^2 = 0.83$ (GdIC12a); nitrate mg/kg; oxalate mg/kg; Fe wt% calcine solids						
Coefficients	I	a	b	c	d	e	f
	0.8935	-0.05003	-0.1814	-0.2779	1.265E-5	-7.972E-6	-0.01756
Glycolate Destruction (Scaled Runs)	Glycolate Destruction $= I + a(AS)$ $R^2 = 0.79$ (GdIC17a)						
Coefficients	I	a					
	0.5291	-0.3409					
Glycolate to Formate Conversion (without noble metals and Hg)	Glycolate to Formate $= I + a(HSV) + b(AS) + c(PRA)$ $R^2 = 0.94$ (Gf3a)						
Coefficients	I	a	b	c			
	-47.47	46.54	-0.8947	-1.0166			

The Acid Calculation spreadsheet will need to be modified to include these equations. Because the Percent Reducing Acid is an output of the acid calculation (to calculate REDOX) and an input to these prediction equations, this variable will necessarily require an iterative solution. The calculation process is shown in Figure 3-25. The new calculation method requires that N_R (N_C) and G_D be calculated from PRA as part of the iterative process, whereas previously N_C and G_D would just be assumed (educated guess) values. Calculation of PRA has always been iterative in the Acid Calculation spreadsheet.

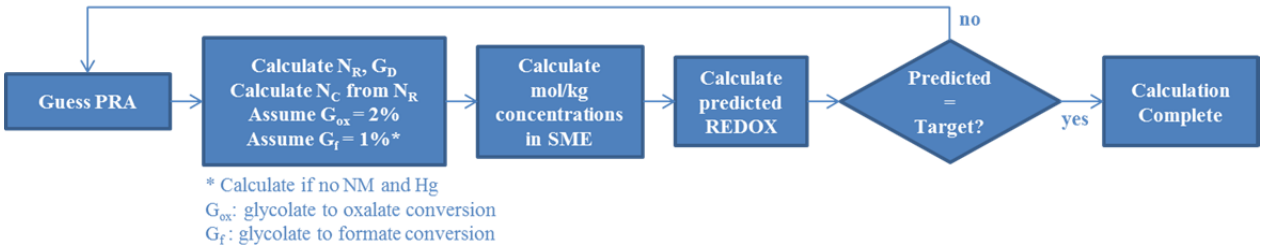

Figure 3-25. Calculation Flowsheet for REDOX Prediction

Use of the predication equations in DWPF will require further work to determine if the correlations that apply to simulant testing work for actual plant radioactive processing. It is expected that the equations for DWPF would be similar to those found for simulant testing. Some differences between the simulant testing and actual plant operation that could make the correlations different are:

1. Presence of heels in the SRAT and SME.
2. Additions of Actinide Removal Process products and Strip Effluent.
3. Differences in the internal refluxing of nitric acid in DWPF versus simulant tests.
4. Differences in the detailed timing of acid additions, concentration, and refluxing (e.g., delay times, acid addition rates, boilup rates).

4.0 Conclusions

1. The N_R formulation of nitrite to nitrate conversion (% final nitrate/all nitrogen inputs) gave better correlation versus the proposed variables than the N_C formulation (nitrite to nitrate conversion). The nitrite to nitrate conversion N_C can be calculated from N_R.
2. The fit of the N_R data for All Data except Uncertain was essentially the same as the fit of only the Scaled Runs data.
3. The nitrite to nitrate conversion is lower in the larger vessels tested that had lower values of HSV and SASV. These results imply there may be more internal refluxing of nitric and nitrous acids in the 4-L vessels compared the larger test vessels (and to DWPF).
4. A headspace specific variable was needed to correlate the data.
5. Either headspace variable ‘headspace volume to sludge volume’ (HSV) or ‘headspace surface area to sludge volume’ (SASV) can be used to correlate data about equally well.
6. Models with quadratic terms fit data better, but adding too many terms appears to fit the data better at the expense of actual physical meaning.
7. For all data sets fit, the ‘Uncertain’ older data from runs GN34-38 were not easily modeled with the proposed variables due to what appears to be significant analytical error. The final models proposed were based on the data without these ‘Uncertain’ data.
8. Because the models did not cover a wide range of realistic sludges, they may not give good results for sludges with compositions significantly different from those modeled.
9. In the model for glycolate destruction, the significant variables nitrate and Fe could probably be substituted by nitrite and Mn, respectively, and achieve similar fits of the data since nitrite and nitrate, and Fe and Mn, are somewhat correlated in the realistic sludges studied.
10. Glycolate destruction was primarily a function of Acid Stoichiometry and Fe content, with Percent Reducing Acid, HSV, nitrate and oxalate being lesser contributors to the fit of the data.
11. Glycolate conversion to formate in the presence of noble metals and mercury averages about 1% with a range of about 0-2%.

12. Glycolate conversion to formate is significantly higher when noble metals and mercury are absent. From 40-100% of the glycolate destroyed with NM and Hg absent is converted to formate.
13. Glycolate conversion to oxalate data were somewhat inconclusive because it appears that upon prolonged storage, glycolate may decompose to oxalate. Glycolate conversion to oxalate of about 2% is recommended.
14. Using the 95% confidence intervals for individual outcome values for glycolate destruction and nitrite to nitrate conversion, the predicted REDOX value for a specific example (GN70) gave an approximate 95% confidence on an individual measured REDOX value of 0.11 with an uncertainty of about ±0.11. Similar uncertainty would be expected for other run data. Note that the uncertainties inherent in the REDOX model are not included in these values.

5.0 Recommendations and Path Forward for Future Work

5.1 Future Development of Models by SRNL

1. Add the bounding hydrogen runs GN80-83 data to the database and re-regress the data.
2. Use the N_R nitrite to nitrate conversion model for SB9. Test both the All Data without Uncertain correlation and the Scaled Runs data correlation since SB9 is similar to SB8.
3. Use both the All Data without Uncertain and Scaled Runs glycolate destruction (from IC) correlations for SB9 predictions.
4. Add SB9 data to the models and re-regress and use for further predictions.
5. Develop SB9-specific models for comparison as sufficient SB9 data are acquired.
6. Perform SB9 runs, as possible, to push the limits of the available variables (sludge non-composition variables; e.g., acid stoichiometry, percent reducing acid).
    a. Consider composition adjustments (e.g., nitrite, nitrate, oxalate) if possible.
    b. Perform runs at KMA acid stoichiometries lower than 100%.
7. Begin the development of a true acid stoichiometry equation that reflects the greater reducing capacity of glycolic acid compared to formic acid. Compare this new equation to the Koopman minimum acid and Hsu acid requirement equations. (See Section 5.3)

5.2 Long Term Use of Models

1. Determine if the older glycolate destruction data are useful in the models or if only newer data with more realistic sludge batch compositions should be used.
2. Continue use of models in future sludge batches and make evolutionary improvements as more data are acquired.
3. Compare model predictions for simulant tests to actual DWPF results.

5.3 Improved Understanding of CPC Chemistry

The KMA acid stoichiometry values are known to be lower than what the actual stoichiometry of the flowsheet is in terms of glycolic acid (e.g., KMA=100% is probably more like 125% acid). The definition of what 100% acid means for the nitric-glycolic flowsheet must be determined or defined. For the formic nitric flowsheet, 100% acid is mainly defined to be the amount of acid that will destroy 100% of the nitrite and reduce all mercury and Mn in addition to completing the acid-base reactions. For the GN

flowsheet, this may still be the appropriate definition, but the actual quantity and balance of acids required will be different because of the different reactions of glycolic acid versus formic acid. It appears that the 100% acid amount for the GN flowsheet may mathematically be about 85% KMA.

Because the generation of significant amounts of hydrogen has never been seen with the GN flowsheet, the need to destroy all nitrite in the SRAT so that the hydrogen does not peak in the SME is no longer necessary. Instead, processability issues such as mercury recovery, slurry rheology, or glass quality may be used to define the allowable limits. Therefore, these and other parameters should be measured and correlated with the acid stoichiometry and other variables much like the nitrite to nitrate conversion and glycolate destruction. The solubility of metals such as Mn, Ni, and Fe should be included in this work.

The following anecdotal observations have been made about the GN flowsheet CPC tests.

1. High acid results in much more viscous slurries.
2. High acid may result in poor glass quality due to higher than expected REDOX.
3. Low acid may also result in more viscous slurries.
4. Higher acid gives better mercury recovery in the Mercury Water Wash Tank.

Specific Recommendations for SB9:

1. Push the bounds of acid stoichiometry lower to where the real 100% acid value is found. This may require performing runs where not all nitrite is destroyed nor all mercury reduced.
2. Push the bounds of glass REDOX lower and higher than the acceptable region to improve the understanding of what compositions produce acceptable glasses.

Simplified chemistry tests are also recommended to better understand the behavior of specific species with glycolic acid. Such tests could include single component (e.g., Mn or Hg) or reduced number of component tests. Tests should also be designed to gain a better understanding of why hydrogen is not formed in the presence of noble metals and mercury when it is known that in their absence large quantities of formate are generated.

6.0 References

1. T.L. White, D.P. Lambert, J.R. Zamecnik, and W.T. Riley, "Ion Chromatography (IC) Analysis of Glycolate in Simulated Waste," **SRNL-STI-2015-00049, Rev. 0**, 2015.

2. JMP Pro Version 11.2.1 or JMP Version 11.2.0, SAS Institute, 2013.

3. D.C. Koopman, D.R. Best, and B.R. Pickenheim, "SRAT Chemistry and Acid Consumption During Simulated DWPF Melter Feed Preparation," **WSRC-STI-2008-00131**, 2008.

4. J.D. Newell, D.P. Lambert, J.R. Zamecnik, and C.J. Martino, "Impact of Scaling on the Nitric-Glycolic Acid Flowsheet," **SRNL-STI-2014-00306, Rev. 0**, 2016.

Appendix A. Anion Analyses

Run Number	SRAT or SME	Nitrate mg/kg	Glycolate mg/kg	Oxalate mg/kg	Formate mg/kg
GN34b	SRAT	57000	46800	6690	467
GN34c	SRAT	54350	51250	7485	285
GN35	SRAT	45700	38800	17600	688
GN36 SME	SME	51572	41353	7420	395
GN 36 SRAT	SRAT	66900	48200	9550	682
GN36b	SRAT	55450	51800	5780	338
GN36c	SRAT	55300	53550	6050	279
GN37	SME	38450	30700	2830	1855
GN37b	SRAT	52950	50650	4760	273
GN38	SRAT	60600	57400	4810	435
GN40	SRAT	55674	47893	15668	516
GN41	SME	48477	45248	17623	332
GN43	SRAT	64900	42100	1440	790
GN44	SRAT	53875	35175	5603	2240
GN45	SRAT	56100	47500	2010	1040
GN46	SRAT	53500	44300	5980	550
GN47	SME	45911	38604	3798	213
GN48	SME	40099	42552	4395	198
GN49	SME	51215	33832	4005	172
GN50	SME	57377	32885	3540	109
GN51	SME	45729	34641	1227	3853
GN52	SME	48144	35485	1037	3887
GN53	SME	58286	45344	1262	2056
GN54	SME	47850	31356	1132	4221
GN54	SME	55600	32425	1245	4565
GN55	SME	55600	32425	1245	4565
GN56	SME	58000	33150	826	7015
GN57	SME	57950	35875	3640	186
GN58	SME	67400	41300	1050	0
GN59	SME	68600	37950	1120	463
GN70	SME	49200	47500	3340	918
GN71	SME	58100	52500	2620	501
GN72	SME	50700	39500	3660	1090
GN73	SME	50600	40300	2600	347
GN74	SME	39700	37900	1780	440
GN75	SME	53800	42300	2630	305
GN76	SME	38300	37500	3690	1640
GN77	SME	48300	39000	2960	258
GN78	SME	51900	43300	2830	108
GN79	SME	41800	38700	3040	313

Appendix B. Summary of Calculations of HSV and SASV

Summary of HSV and SASV Values:

	total head space surface area		sludge mass		sludge volume		**surface area to sludge volume ratio**		total headspace volume		**headspace to sludge volume ratio**
GN70-75	1,380	cm^2			3,037	mL	**0.454**	cm^{-1}	3,070	mL	**1.011**
GN76	1,655	cm^2			17,602	mL	**0.094**	cm^{-1}	6,959	mL	**0.395**
GN77	1,904	cm^2			15,872	mL	**0.120**	cm^{-1}	8,689	mL	**0.547**
GN78	12,378	cm^2			114,865	mL	**0.108**	cm^{-1}	101,994	mL	**0.888**
GN79	11,069	cm^2			134,149	mL	**0.083**	cm^{-1}	82,710	mL	**0.617**
GN34b	1,456	cm^3	3,174	g	2,784	mL	**0.523**	cm^{-1}	3,323	mL	**1.194**
GN34c	1,455	cm^2	3,178	g	2,788	mL	**0.522**	cm^{-1}	3,320	mL	**1.191**
GN35	1,457	cm^3	3,169	g	2,780	mL	**0.524**	cm^{-1}	3,327	mL	**1.197**
GN36	1,456	cm^3	3,173	g	2,783	mL	**0.523**	cm^{-1}	3,324	mL	**1.194**
GN36b	1,456	cm^3	3,173	g	2,783	mL	**0.523**	cm^{-1}	3,324	mL	**1.194**
GN36c	1,456	cm^3	3,173	g	2,783	mL	**0.523**	cm^{-1}	3,324	mL	**1.194**
GN37	1,456	cm^3	3,174	g	2,784	mL	**0.523**	cm^{-1}	3,323	mL	**1.194**
GN37b	1,449	cm^3	3,200	g	2,807	mL	**0.516**	cm^{-1}	3,300	mL	**1.176**
GN38	1,446	cm^3	3,209	g	2,815	mL	**0.514**	cm^{-1}	3,292	mL	**1.170**
GN40	1,421	cm^3	3,306	g	2,900	mL	**0.490**	cm^{-1}	3,207	mL	**1.106**
GN41	1,421	cm^3	3,306	g	2,900	mL	**0.490**	cm^{-1}	3,207	mL	**1.106**
GN43	1,507	cm^3	2,980	g	2,614	mL	**0.576**	cm^{-1}	3,493	mL	**1.336**
GN44	1,507	cm^3	2,980	g	2,614	mL	**0.576**	cm^{-1}	3,493	mL	**1.336**
GN45	1,507	cm^3	2,980	g	2,614	mL	**0.576**	cm^{-1}	3,493	mL	**1.336**
GN46	1,507	cm^3	2,978	g	2,612	mL	**0.577**	cm^{-1}	3,495	mL	**1.338**
GN47	1,382	cm^3	**3,454**	g	3,030	mL	**0.456**	cm^{-1}	3,077	mL	**1.016**
GN48	1,382	cm^3	**3,454**	g	3,030	mL	**0.456**	cm^{-1}	3,077	mL	**1.016**
GN49	1,382	cm^3	3,455	g	3,031	mL	**0.456**	cm^{-1}	3,077	mL	**1.015**
GN50	1,382	cm^3	3,455	g	3,031	mL	**0.456**	cm^{-1}	3,077	mL	**1.015**
GN51	1,399	cm^3	3,389	g	2,973	mL	**0.471**	cm^{-1}	3,134	mL	**1.054**
GN52	1,399	cm^3	3,389	g	2,973	mL	**0.471**	cm^{-1}	3,134	mL	**1.054**
GN53	1,400	cm^3	**3,385**	g	2,969	mL	**0.472**	cm^{-1}	3,138	mL	**1.057**
GN54	1,399	cm^3	3,389	g	2,973	mL	**0.471**	cm^{-1}	3,134	mL	**1.054**
GN55	1,399	cm^3	3,389	g	2,973	mL	**0.471**	cm^{-1}	3,134	mL	**1.054**
GN56	1,399	cm^3	**3,388**	g	2,972	mL	**0.471**	cm^{-1}	3,135	mL	**1.055**
GN57	1,394	cm^3	3,409	g	2,990	mL	**0.466**	cm^{-1}	3,117	mL	**1.042**
GN58	1,399	cm^3	3,388	g	2,972	mL	**0.471**	cm^{-1}	3,135	mL	**1.055**
GN59	1,399	cm^3	3,389	g	2,973	mL	**0.471**	cm^{-1}	3,134	mL	**1.054**
DWPF	284,376	DWPF			31,570,236	mL	**0.00901**	cm^{-1}	12,976,730		**0.411**
220L	12,378	GN78			114,865	mL	**0.108**	cm^{-1}	101,994		**0.888**
220L	11,069	GN79			134,149	mL	**0.0825**	cm^{-1}	82,710		**0.617**
22L	1,655	GN76		0.1070	17,602	mL	**0.0940**	cm^{-1}	6,959		**0.395**
22L	1,904	GN77			15,872	mL	**0.120**	cm^{-1}	8,689		**0.547**
4-L	1,380	GN70-75		0.495	3,037	mL	**0.454**	cm^{-1}	3,070		**1.01**
4-L	1,454	GN34-38			2,790	mL	**0.521**	cm^{-1}	3,318		**1.19**
4-L	1,421	GN40-41			2,900	mL	**0.490**	cm^{-1}	3,207		**1.11**
4-L	1,507	GN43-46			2,614	mL	**0.576**	cm^{-1}	3,493		**1.33**
4-L	1,382	GN47-50			3,030	mL	**0.456**	cm^{-1}	3,077		**1.02**
4-L	1,399	GN51-59			2,974	mL	**0.470**	cm^{-1}	3,133		**1.05**

Distribution:

T. B. Brown, 773-A
M. E. Cercy, 773-42A
D. A. Crowley, 773-43A
D. E. Dooley, 773-A
A. P. Fellinger. 773-42A
S. D. Fink, 773-A
C. C. Herman, 773-A
D. T. Hobbs, 773-A
E. N. Hoffman, 999-W
J. E. Hyatt, 773-A
K. M. Kostelnik, 773-42A
B. B. Looney, 773-42A
D. A. McGuire, 773-42A
T. O. Oliver, 773-42A
F. M. Pennebaker, 773-42A
G. N. Smoland, 773-42A
A. L. Washington, 773-42A
W. R. Wilmarth, 773-A
Records Administration (EDWS)

H. P. Boyd, 704-27S
J. M. Bricker, 704-S
J. S. Contardi, 704-56H
T. L. Fellinger, 766-H
E. J. Freed, 704-S
J. M. Gillam, 766-H
B. A. Hamm, 766-H
E. W. Holtzscheiter, 766-H
J. F. Iaukea, 704-27S
V. Jain, 766-H
C. J. Martino, 999-W
J. W. Ray, 704-27S
P. J. Ryan, 704-26S
M. A. Rios-Armstrong, 766-H
H. B. Shah, 766-H
D. C. Sherburne, 249-8H
C. Sudduth, 707-7E

P. R. Jackson, DOE-SR, 703-46A
J. A. Crenshaw, 703-46A

D. P. Lambert, 999-W
J. D. Newell, 999-W
M. S. Williams, 999-W
C. M. Jantzen, 773-A
H. L. Watson, 773-42A
T. E. Smith, 999-W
M. E. Stone, 999-W